

Universidade do Minho
Escola de Ciências

Mário Ismael Cardoso Fernandes

**Development of nanocarriers for Alzheimer's
disease treatment**

Mário Ismael Cardoso Fernandes **Development of nanocarriers for Alzheimer's disease treatment**

UMinho|2019

janeiro de 2019



Universidade do Minho
Escola de Ciências

Mário Ismael Cardoso Fernandes

Development of nanocarriers for Alzheimer's disease treatment

Tese de Mestrado

Mestrado em Biofísica e Bionanossistemas

Trabalho efetuado sobre a orientação de

Doutora Cláudia Manuela Cunha Ferreira Botelho

Professora Doutora Andreia Ferreira de Castro Gomes

Janeiro de 2019

Declaração

Nome: Mário Ismael Cardoso Fernandes

Endereço eletrónico: pg31417@alunos.uminho.pt

Contacto telefónico: 916230234

Cartão de cidadão: 14827526

Título da dissertação: “Development of nanocarriers for Alzheimer’s disease treatment”

Orientadores: Doutora Cláudia Botelho e

Professora Doutora Andreia Gomes

Ano de conclusão: 2019

Mestrado em Biofísica e Bionanossistemas

DE ACORDO COM A LEGISLAÇÃO EM VIGOR, NÃO É PERMITIDA A REPRODUÇÃO DE
QUALQUER PARTE DESTA DISSERTAÇÃO

Universidade do Minho, ___/___/_____

Assinatura_____

Acknowledgments

Gostaria de agradecer à Professora Doutora Andreia Gomes por todo o suporte, ajuda e paciência ao longo deste projeto. Agradeço sempre pelo exemplo fantástico dado de profissionalismo e dedicação. Gostaria também de agradecer toda a disponibilidade, e todos os conselhos dados, toda a energia, toda a força, e todos os ensinamentos, os quais me fizeram crescer como pessoa e como investigador.

Queria também agradecer à Doutora Cláudia Botelho pela disponibilidade e por todos os conselhos dados, pela paciência e pela ajuda prestada ao longo do ano. Agradeço a dedicação e sabedoria disponibilizados para elaboração desta tese.

Agradeço também ao Ivo por tudo o que me ensinou, pela introdução à vida laboratorial, por todo o tempo disponibilizado, e por toda a paciência. Agradeço também a sua ajuda constante, e o facto de ter sempre as “portas abertas” para o esclarecimento de todas as dúvidas, ou para ajudar com qualquer tarefa.

À Anabela pelo seu acompanhamento e pela sua amizade. Pela sua ajuda não só no meu trabalho laboratorial como em tudo o que demais é importante na “vida laboratorial”. Obrigado pela disponibilidade, frontalidade e sinceridade.

Agradeço aos meus colegas de laboratório: à Rita, à Sara, ao Jorge, Diogo e Hélder pela companhia, pelos bons momentos e por me ajudarem em todos eles e serem importantes para a realização deste percurso. Agradeço também à Rita Nunes pela companhia e pelos bons momentos partilhados. Um agradecimento especial ao Pedro por todo o tempo disponibilizado, por todos os bons momentos, pela companhia e pelo apoio constante nos piores e melhores momentos.

Por fim agradeço aos meus pais por serem absolutamente essenciais neste processo. Por serem compreensivos e serem sempre os melhores exemplos, pelos quais me tentei guiar. Obrigado pelo apoio, pela dedicação e por toda a força dada e por serem verdadeiros heróis no suporte que me foi dado.

Resumo

Desempenhando um papel central em todas as funções do corpo, o cérebro é talvez o órgão mais bem protegido em todo o corpo. Embora isso seja uma enorme vantagem, devido a todos os patógenos perigosos e moléculas prejudiciais que poderiam colocar a sua integridade em risco, este torna-se assim também num órgão muito difícil de intervencionar em termos clínicos. Terapeuticamente, o primeiro passo limitante para entregar uma substância ativa no cérebro é a passagem dessa molécula através da barreira hematoencefálica.

Embora esteja bem protegido, o cérebro não é imune a todos os distúrbios, uma vez que algumas das moléculas envolvidas nas patologias mais graves, tais como as proteínas A β -amiloide e TAU na doença de Alzheimer, e alfa-sinucleína na doença de Parkinson, parecem ser produzidas no próprio cérebro. Além disso, essas doenças têm outra característica em comum: a acumulação de espécies reativas de oxigênio no cérebro.

Com o encapsulamento de siRNA contra a proteína TAU em lipossomas do tipo exossomal, pretendemos reduzir a expressão dessa proteína, cuja acumulação em células nervosas é uma característica da doença de Alzheimer. Além disso, o encapsulamento de uma molécula com propriedades antioxidantes, como a curcumina, poderá contribuir para a diminuição da acumulação de β -amiloide no cérebro, contribuindo para uma progressão mais lenta desta doença.

Foi conseguido, com sucesso, o encapsulamento de ambas as moléculas nos lipossomas miméticos de exossomas, com eficiências de encapsulamento elevadas. Conseguida a otimização da formulação para garantir que os lipossomas produzidos têm o tamanho necessário para conseguir ultrapassar a barreira hematoencefálica, também se verificou que os lipossomas vazios ou carregados com curcumina não apresentavam toxicidade significativa em duas linhas celulares: fibroblastos de ratinho L929 e linha celular de neuroblastoma humano SH-SY5Y. Adicionalmente demonstramos que curcumina veiculada em lipossomas tinha efeito neuroprotetor maior do que a curcumina livre, após a indução de stress oxidativo.

Abstract

Playing a central role in all the body's functions, the brain is perhaps the best protected organ in the organism. Although this is a huge advantage before all potential pathogens and harmful molecules that could put its integrity at risk, it is also a very difficult organ to target therapeutically. Being highly selective to all molecules, the blood brain barrier is the primary and most difficult barrier to overcome when one aims to deliver a specific molecule to the brain.

While it is well protected, the brain is not immune to disease, and some of the molecules involved in the most threatening disorders, like amyloid- β and TAU in Alzheimer's disease, and alpha-synuclein in Parkinson's disease, are thought to be produced in the brain itself. Moreover, these diseases have another hallmark in common, which is the accumulation of reactive oxygen species in the brain. This happens because, being a highly energy demanding organ, the brain is the most metabolically active organ in the human body.

In order to overcome these two major debilitating hallmarks, a dual therapy is being developed by our group. By encapsulating siRNA against TAU protein into exosome-like liposomes we aim to reduce its expression, diminishing its harmful effects due to excessive accumulation in neurons, in Alzheimer's disease. Furthermore, the encapsulation of a molecule with antioxidant properties, such as curcumin, that reduces the accumulation of amyloid- β , another important hallmark in this disease, would most likely have considerably interesting results in the attempt to slow disease progression.

For the encapsulation of these molecules, a liposome carrier, with similar constitution and properties of the exosomes, was chosen. Along with its low cytotoxicity verified in two cell lines, mouse L929 fibroblasts and human neuroblastoma SH-SY5Y cells, this carrier has features compatible with the uptake across the blood brain barrier and therefore could directly influence disease progression. It was also found that curcumin-loaded liposomes had greater neuroprotective effects than free curcumin after induction of oxidative stress.

Table of contents

Declaração.....	ii
Acknowledgments	iii
Resumo	iv
Abstract	v
Table of contents.....	vi
Figure Index	ix
Table Index	xi
Equation index	xii
1. Introduction	1
1.1 Neurodegenerative disorders.....	1
1.2 Alzheimer´s disease	1
1.3 Oxidative stress.....	3
1.4 Amyloid- β production.....	5
1.5 Tau phosphorylation and neurofibrillary tangles (NFTs)	7
1.6 Diagnosis and treatment of Alzheimer	9
1.7 Blood brain barrier – the mediator of molecule internalization into the brain.....	11
1.8 Blood brain barrier intake pathways.....	11
1.9 Nanoparticles: advantages and utility.....	12
1.9.1 Liposomes	13
1.10 Nanocarriers used in the treatment of Alzheimer´s disease	14
1.11 Curcumin properties and effects in Alzheimer´s disease treatment	15
1.12 Gene silencing therapy	16
1.12.1 RNA interference therapy	16
1.13 Exosome composition and formation	18

1.13.1	Therapeutic administration of exosomes	18
1.14	Exosome-like nanoparticles.....	19
1.15	Objetive	20
2	Materials and Methods	20
2.1	Materials	21
2.2	Lipid solutions	21
2.3	Curcumin solution.....	21
2.4	Buffers	22
2.5	Exosome-like liposome preparation.....	22
2.6	Preparation of exosome-like liposomes with DODAP.....	23
2.6.1	Separation of the encapsulated and free fractions	23
2.6.1.1	Exosome-like liposome purification in a molecular exclusion column.....	24
2.6.1.2	Separation of the encapsulated and free fractions of siRNA using amicons®.	24
2.7	Size and polydispersity determination by Dynamic light scattering (DLS)	24
2.8	Surface charge measurement by Electrophoretic light scattering (ELS)	26
2.9	Exosome-like liposome lipid concentration quantification.....	26
2.10	Lysis of the exosome-like liposomes for the quantification of encapsulated siRNA	27
2.11	Encapsulated siRNA quantification.....	27
2.11.1	Quantification of siRNA encapsulation by electrophoresis	29
2.12	Curcumin encapsulation in the samples	29
2.13	Co-encapsulation of siRNA and curcumin in exosome-like liposomes containing	
DODAP	30	
2.14	Curcumin encapsulation efficiency determination.....	30
2.14.1	Fourier-transform infrared spectroscopy (F-TIR).....	31
2.15	Mammalian cell culture	31
2.16	Viability assessment - Resazurin assay.....	32

2.17	Cell membrane integrity - Trypan blue assay	32
2.18	Curcumin neuroprotection assays.....	33
3	Results	34
3.1	Empty and curcumin loaded exosome-like liposomes	34
3.1.1	Size, PDI and zeta potential of empty and curcumin-loaded exosome-like liposomes	35
3.1.2	Storage stability of empty and curcumin-loaded exosome-like liposomes.....	35
3.1.3	Curcumin encapsulation efficiency.....	36
3.1.4	F-TIR assay	37
3.1.5	Resazurin assay	38
3.1.6	Trypan blue assay	40
3.1.7	Curcumin internalization assay	42
3.1.8	Curcumin neuroprotection assay	44
3.1.9	Reactive Oxygen Species (ROS) generation in SH-SY5Y cell line.....	45
3.1.10	Acridine orange/ Propidium iodide assay.....	46
3.2	siRNA exosome-like liposomes.....	49
3.2.1	Size, PDI and zeta potential of siRNA exosome-like liposomes	49
3.2.2	siRNA encapsulation efficiency	50
3.2.3	siRNA and curcumin co-encapsulation efficiency	53
4	Discussion	55
4.	Bibliography	59
5.	Supplementary Data	75

Figure Index

Figure 1: Alzheimer's disease most important hallmarks.	3
Figure 2: Oxidative stress causes and neuronal damage associated with ROS uncontrolled production and accumulation.....	4
Figure 3: Amyloid- β production.....	5
Figure 4: Progression of TAU pathology.....	8
Figure 5: Exosome components and lipidic constitution cholesterol (CHOL); sphingomyelin (SM); phosphatidylcholine (PC); phosphatidylserine (PS) and phosphatidylenitol (PE).....	18
Figure 6: Schematic representation of a dip cell. Adapted from ^[127]	26
Figure 7: siRNA calibration curve.	28
Figure 8: Curcumin calibration curve.	30
Figure 9: Size, polydispersity and zeta potential of empty and curcumin-loaded exosome-like liposomes, with and without DODAP.....	35
Figure 10: Stability of empty exosome-like liposomes without DODAP.....	36
Figure 11: Stability of empty exosome-like liposomes with DODAP.....	36
Figure 12: F-TIR absorbance spectra of free curcumin, empty exosome-like liposomes and curcumin-loaded exosome-like liposomes. The black arrows show the peaks where the presence of the exosome-like liposomes is visible, and the blue arrows indicate the presence of curcumin.....	37
Figure 13: Viability assays of exosome-like liposomes with DODAP. All concentrations of exosome-like liposomes with DODAP induce little to no cytotoxicity. These exosome-like liposomes show little toxicity that does not seem to be correlated with their concentration.....	38
Figure 14: Viability assays of exosome-like liposomes without DODAP; All concentrations of exosome-like liposomes without DODAP induce little to no cytotoxicity. The two most concentrated samples of these exosome-like liposomes seem to induce more toxicity than all the other samples.	39
Figure 15: Cytotoxicity of curcumin-loaded exosome-like liposomes.	40
Figure 16: Percentage of unmarked cells when incubated with exosome-like liposomes with DODAP. The cells were counted, and the percentage was expressed considering the percentage of unmarked in relation to the total number of cells.....	41

Figure 17: Percentage of unmarked cells (viable cells) when incubated with exosome-like liposomes without DODAP. The cells were counted, and the percentage was expressed considering the percentage of unmarked in relation to the total number of cells.	41
Figure 18: Curcumin internalization in SH-SY5Y cells: a), c) and e) 2h of incubation and b); d) and f) 4h of incubation. a) and b) represent free curcumin 20 μM ; c) and d) exosome-like liposomes without DODAP with 20 μM of curcumin and e) and f) exosome-like liposomes with DODAP with 20 μM of curcumin.	43
Figure 19: Effects in cell metabolism when SHSY-5Y cells are incubated with three different concentrations of curcumin (400 μM , 40 μM and 8 μM). The oxidative stress inducer was t-BHP at 1 μM	44
Figure 20: Neuroprotective effects of exosome-like liposomes with curcumin encapsulated. The oxidative stress inducer t-BHP 1 μM	45
Figure 21: Percentage of ROS in each condition. The percentage is expressed relative to the control with t-BHP.	46
Figure 22: Percentage of non-apoptotic cells for each condition.	47
Figure 23: Apoptotic cells incubated with a) only medium; b) medium with t-BHP 1 mM; c) h) free curcumin 20 μM ; d) 20 μM of curcumin loaded exosome-like liposomes without DODAP; e) 8 μM of the previous exosome-like liposomes; f) 20 μM of curcumin loaded exosome-like liposomes with DODAP; g) 8 μM of the previous exosome-like liposomes.	48
Figure 24: Size, polydispersity and zeta potential of exosome-like liposomes without DODAP and with rising concentrations of siRNA (C1=4.1x10 ⁻⁶ M; C2=5x10 ⁻⁶ M; C3=1x10 ⁻⁵ M e C4=2x10 ⁻⁵ M).	49
Figure 25: Exosome-like liposomes with the initial formulation in Hepes buffer with a siRNA concentration of 4.1x10 ⁻⁵ M after heating, vortexing, and cooling 5 min on ice: a) exosome-like liposomes without detergent; b) exosome-like liposomes with C12E8; c) with Tween 20 and d) with Triton 10x.	50
Figure 26: Electrophoresis of: a) siRNA 3.32 μg ; b) sample without purification; c) free part; d) encapsulated part; e) purified and treated with detergent; f) unpurified exosome-like liposomes; g) free part; h) encapsulated part; i) purified and treated with detergent exosome-like liposomes; j) ladder.	52
Figure 27: Electrophoresis of a) siRNA 3.32 μg ; b) sample without purification; c) free part; d) encapsulated part; e) encapsulated part treated with C12E8; f) encapsulated part treated with Triton	

10x; g) purified exosome-like liposomes; h) purified and treated C12E8 exosome-like liposomes; i) purified and Triton-treated exosome-like liposomes; j) ladder..... 53

Figure 28: Electrophoresis of: a) siRNA; exosome-like liposomes with DODAP b) without siRNA; c) non-purified; d) non-purified with C12E8; e) purified; f) purified with C12E8; g) encapsulated part; h) C12E8-treated encapsulated part; i) free siRNA from the exosome-like liposomes passed through the amicon®; j) ladder. 54

Figure 29: L929 cell morphology after 24 h of incubation with the exosome-like liposomes. 75

Table Index

Table 1: Nanocarriers used in the treatment of Alzheimer's disease and the encapsulated molecules..... 14

Table 2: Concentration of the stock solution and percentage of the various lipids used in the preparation of the exosome-like liposomes. 22

Table 3: Curcumin encapsulation efficiency of samples with and without DODAP in the formulation ($\lambda_{exc}=420nm$; $\lambda_{em}=520nm$). 37

Table 4: Encapsulation efficiency of 3 different siRNA concentrations in the exosome-like liposomes with DODAP. 51

Table 5: Encapsulation efficiency of curcumin 1×10^{-3} M and 4.1×10^{-5} M siRNA in exosome-like liposomes with DODAP. 54

Equation index

Equation 1: Stokes-Einstein equation where K_b is the Boltzmann constant, T is the absolute temperature, D is the particle's hydrodynamic diameter and μ is the dynamic viscosity of the medium	25
Equation 2: Relationship between the number of moles of siRNA and the number of moles of the lipid in solution	28
Equation 3: Efficiency of encapsulation of siRNA in the liposomes. After the calculation of the theoretical and experimental percentage of siRNA, we can calculate the percentage of siRNA encapsulated in the liposomes by dividing the experimental value by the theoretical value of siRNA..	28
Equation 4: Encapsulation efficiency of curcumin. The fluorescence of the purified liposomes $[\text{curcumin}]_p$ is divided by the fluorescence of liposomes without purifying $[\text{curcumin}]_r$, after the utilization of a calibration curve with increasing concentrations of curcumin incubated with empty liposomes.....	31

1. Introduction

1.1 Neurodegenerative disorders

Neurodegenerative disorders are characterized by the progressive changes in cognition, emotions and behavior. In 2010, approximately 35.6 million people were affected by neurodegenerative diseases in the worldwide^[1].

The available therapies for this type of diseases have poor efficiency^[2]. Therefore, it is predicted that without more efficient treatment, the number of people suffering from neurodegenerative diseases will rise exponentially in the next years^[3].

Moreover, age-related neurodegenerative disorders including, Alzheimer's disease, Parkinson's disease, amyotrophic lateral sclerosis and frontal dementia are the major cause of disability and premature death among elder people around the globe. The severity of these diseases, which includes significant loss of cognitive and motor functions leads to a poor quality of life of the patient and also to their relatives. In spite of the differences between these diseases, they all have a common hallmark: the accumulation of specific proteins into insoluble aggregates in selectively vulnerable neurons and glial cells^[4].

The onset of these diseases is the neuronal damage by specific proteins and oxidative stress^[5], leading to problems within the normal function of synaptic transmission. These diseases' initial damage is normally associated with axonal and dendritic degeneration. Neuron degeneration, associated with self-renewal brain cell's deterioration, due to normal aging and the disease has an important role in all neurodegenerative diseases^[1].

1.2 Alzheimer's disease

Alzheimer's disease is the most common neurological age-dependent neurodegenerative disorder. The number of people affected by this disease is already very high and tends to increase in the future, due to an ever-increasing number of elderly people^[6]. Furthermore, it is thought that this

number will not increase linearly, but in an exponential way. In 2016, there were 44 million people diagnosed with Alzheimer and the in the year 2050, it is expected that 1 in 85 people worldwide will be affected with this disease.

It was estimated that in 2015 the cost of the treatments associated with Alzheimer was around 226 billion dollars and it is expected that in 2050 this number it will reach 1.1 trillion dollars^[7]. To the date, there is no cure for Alzheimer 's disease; the treatment is focused on the relief of the patient's symptoms^[8]. Even so, most of the therapeutic drugs used are inefficient. The main cause for the inefficiency of the current treatments is the difficulty to deliver the molecules to the brain.

In the brain, communication between neurons is made at the synapses, by neurotransmitters. In Alzheimer's disease this process is compromised, either by the deterioration of neurons or the inefficient "sharing of information" in the synaptic cleft^[9].

Alzheimer's disease is characterized by an initial progressive loss of pyramidal neurons, primarily within the cerebral cortex and in the hippocampus^[10].

This disease leads to the loss of the ability to form new memories, or to recall old ones^[7]. Other important symptoms associated with this disorder include dementia, impairment of opinion, language, learning and abstract thinking^[8].

Alzheimer 's disease cause is not clear, although it may be related to environmental factors and genetic pre-disposition^{[11]-[13]}. Early-onset Alzheimer's disease (diagnosed before the age of 65), is rare, as it corresponds only to 10% of all Alzheimer's cases^[14]. This fact implies that age is an important factor on the development of Alzheimer's^{[15]-[17]} With ageing, the brain functions deteriorate making it more susceptible to the disease. Even though there have been many different opinions regarding the most important triggers for the development of this disease, most agree that TAU phosphorylation, mitochondrial dysfunction, mutations in various genes, amyloid β accumulation and oxidative stress, and other external factors (**Figure 1**) play a major role in this disease.

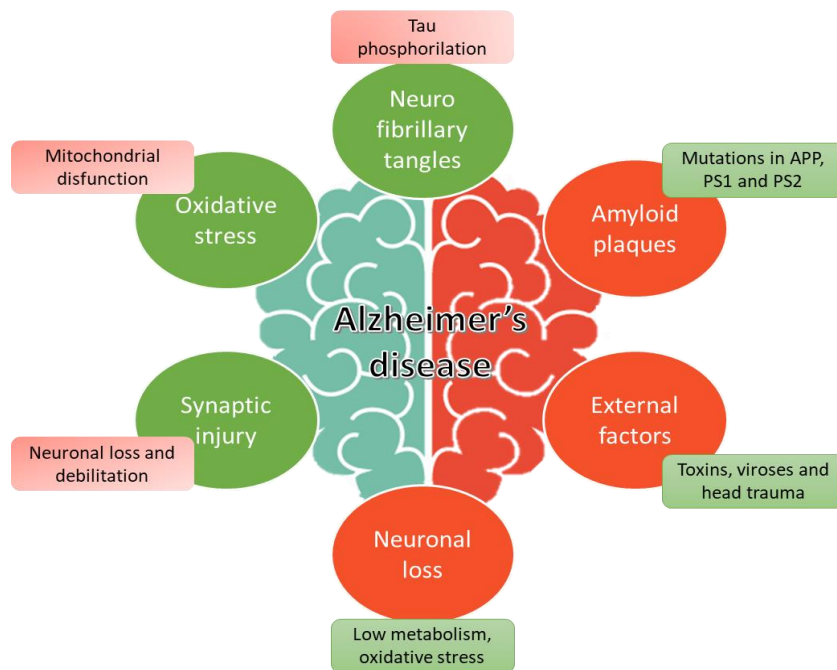


Figure 1: Alzheimer's disease most important hallmarks.

1.3 Oxidative stress

The brain is one of the most metabolically active organs, demanding a high energy production, consuming up to 25% of glucose, with a tight control of the surrounding environment^[18]. In fact, despite representing only 2% of the body weight, the brain is responsible for the consumption of up to 20% of the energy produced by the human body^[19]. This can be explained by the high need of ATP for the neurons, for them to be able to maintain their membrane potential and for the packing and release of neurotransmitters. Despite its poor capacity for storing energy, the brain is always receiving a constant supply of energy substrates, mainly glucose. Glucose overcomes the blood brain barrier through the glucose transporter 1 (GLUT1). For this reason, the cardiac blood input to the brain is usually up to 15% of the total blood consumption. An important part of the total oxygen consumption is done by the endothelial cells, which have a high ATP production. These cells are rich in mitochondria and nicotinamide adenine dinucleotide phosphate (NADPH) oxidases, and so the brain is highly susceptible to oxidative stress damage^[20].

A small concentration of ROS is beneficial, as it is required for the brain cells' functions. ROS can act as vasodilator and it is involved in the regulation of signal transduction. The presence of ROS is important for the immune defense system and on the induction of mitogenic responses. However,

a dysregulation of the production and/or elimination of this molecule can lead to severe consequences for several brain functions. For example, an increase in ROS production reduces the immune system defenses, induces the production of pro-apoptotic agents and reduces the bioavailability of nitric oxide (NO), that has vasodilator and anti-inflammatory properties. Moreover, ROS overproduction can lead to pericyte apoptosis. These play a major role in blood brain barrier integrity, so the reduction of their viability can lead to extensive damage in this barrier^[20].

Oxidative stress is particularly harmful for the mitochondria, since this organelle is both a producer and a target of hydrogen peroxide and superoxide. These molecules can stimulate lipid peroxidation (figure 2).

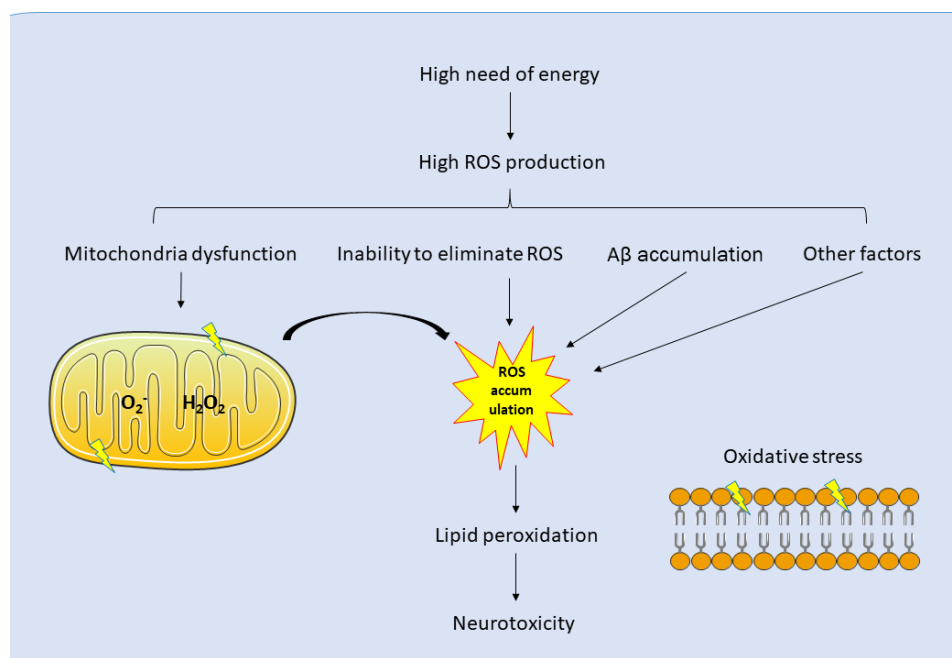


Figure 2: Oxidative stress causes and neuronal damage associated with ROS uncontrolled production and accumulation.

The overproduction of hydrogen peroxide and superoxide can induce the consumption of nicotinamide adenine dinucleotide (NAD) by Poly (ADP-ribose) polymerase (PARP). Thus, the decreasing of NAD can reduce the availability of NADH for complex I in the mitochondria. The ROS production can also inhibit glucose transporters and reduce the amount the substrates available for mitochondria normal function^[21].

1.4 Amyloid- β production

Oxidative stress is normally linked to Alzheimer's disease. The oxidative stress normally precedes the production of amyloid- β protein. Besides that, oxidative stress promotes the production and aggregation of β - β , as well as the enhancement of neurofibrillary tangles polymerization, that are twisted fibers inside neurons.

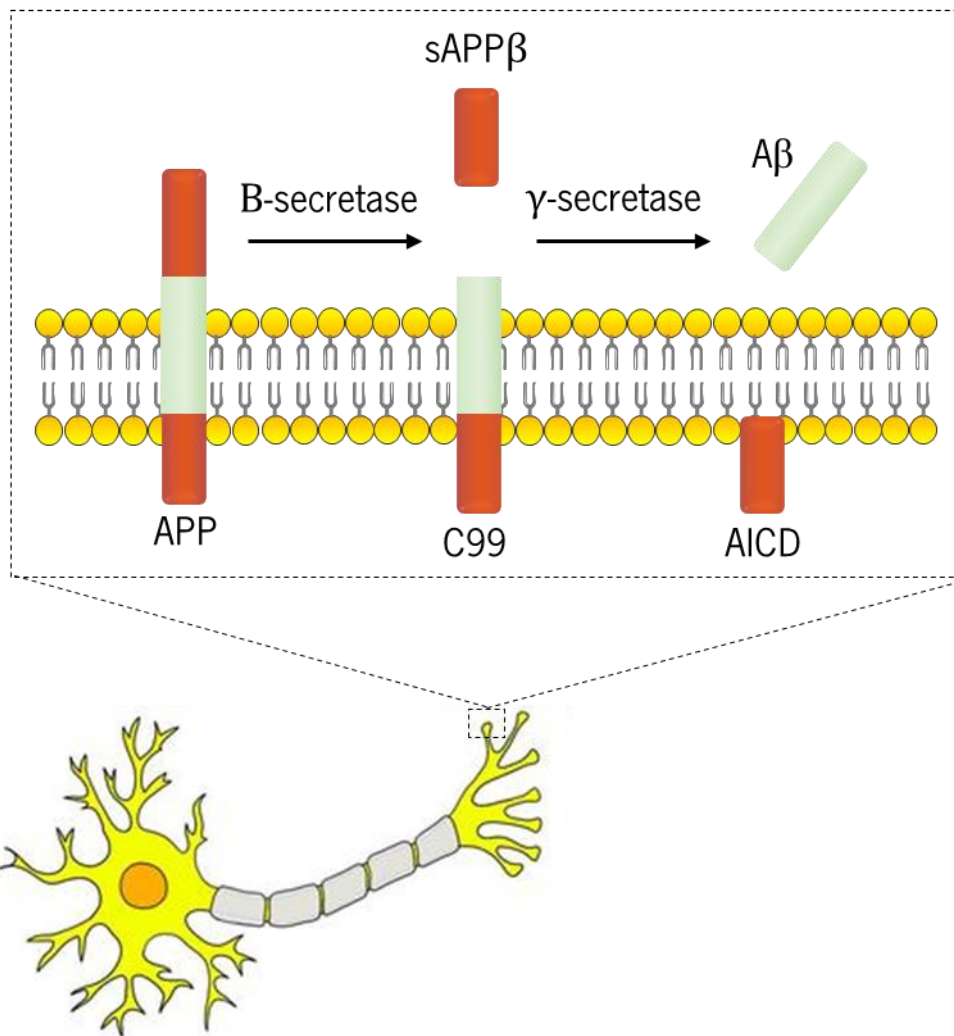


Figure 3: Amyloid- β production.

Amyloid- β has an important role in the progression of this disease. The pathways that are dysregulated resulting in the production of amyloid- β are well studied. Amyloid- β aggregation and deposition, causes synaptotoxicity and it has been considered, for the past 20 years, the main responsible for the development of the disease^[22].

In a normal brain, the amyloid- β is produced in low quantities, outside the cells, or in axon terminals being then degraded or removed. Low doses of this protein can act as a positive regulator of presynaptic activity, enhancing neurotransmitter release and increasing neuron excitability^[23]. However, as the brain ages, the capacity to degrade this protein is reduced. When there is an abnormal production of this protein, and/or a poor degradation, the amyloid- β accumulates and aggregates in oligomers. This accumulation is more frequent in the synaptic cleft, leading to synaptic dysfunction^[24], or along the neuron^[25].

The amyloid- β production starts with the cleavage of the amyloid precursor protein (APP) by β -secretase, followed by another cleavage by the γ -secretase. There are two major types of amyloid- β produced by healthy neural and non-neural cells in the human brain^[26], the A β 40 and A β 42, which have 40 and 42 amino acid residues, respectively. A β 42 is more hydrophobic than A β 40, and tends to aggregate more, due to its size, being considered the most toxic one, and seems to be more associated with cognitive decline than A β 40^{[27],[28]}. An abnormal production of A β 42, or an increase in the ratio A β 42/A β 40 induces amyloid fibril formation, leading to the formation of the senile plaque^[29]. The formation of senile plaques is often linked to tauopathy in Alzheimer's disease, since various studies postulate that the accumulation of senile plaque trigger the production of pTAU^[30].

During the amyloid- β formation there is an initial inflammatory stimulus that triggers microglia at the central nervous system. Microglia secrete various pro-inflammatory cytokines and chemokines that recruit microglia along with astrocytes to the local of inflammation. When the excessive production of amyloid- β occurs, the recruited microglia and astrocytes are not able to degrade the excess of this protein, resulting in a high production of cytokines and chemokines. This results in the deterioration of local neurons, leading to a high progression of Alzheimer^[10].

Amyloid- β peptides exert various types of harmful effects on neurons and other brain cells. In neurons, amyloid- β peptides directly promote neuronal apoptosis by interacting with cell-surface receptors. Long term accumulation of this protein can have more nefarious results, such as the oxidative damage of DNA and proteins, along with physical injury of organelles and the dysregulation of intracellular calcium levels, that can lead to cell death. One of the major problems of Alzheimer's disease is that the deterioration of neurons may not be detectable for years, only showing symptoms when the affected area is extensive^[31].

Amyloid- β is strongly and negatively linked with Alzheimer's disease. However, some recent studies have tried to clarify amyloid- β role in this pathology. As described by Brothers *et al.*, Amyloid- β has beneficial effects, like antibacterial, antifungal, and antiviral properties, being efficient, at least, against eleven types of microbes^[32]. Moreover, it can be important in cancer therapy inhibiting angiogenesis, and in slowing tumor growth^[33]. Interestingly, this protein also has a function in the brain, as it is able to seal leaks in the blood brain barrier, by binding blood-borne solutes together and forming a plug that prevents the spread of neuroactive and toxic components into the brain. This protein also promotes the recovery after brain injury and regulates neurons' synaptic function, as it regulates the responsiveness of glutamatergic and cholinergic synapses in the hippocampus, thus contributing to memory consolidation. These beneficial features can be the reason why this protein has persisted, and it is found in most vertebrates^[34].

1.5 Tau phosphorylation and neurofibrillary tangles (NFTs)

The deposition of neurofibrillary tangles in the brain is an important hallmark in the progression of the disease. Most of the approaches to slow the progression of Alzheimer's disease targeting the amyloid- β protein accumulation have failed. While many consider that amyloid- β is the major player in the development of Alzheimer's disease, the paradigm has changed in the past few years, with accumulated studies that reveal that a reduction of TAU (and a consequent reduction of neurofibrillary tangles) has a higher impact on the disease treatment than the reduction of the amyloid- β protein^[35]. In fact, it has been shown that the reduction of pTAU levels, as amyloid- β continued to increase, improves cognitive function, suggesting that this protein can have a more significant role on the progression of Alzheimer's disease than amyloid- β ^[36].

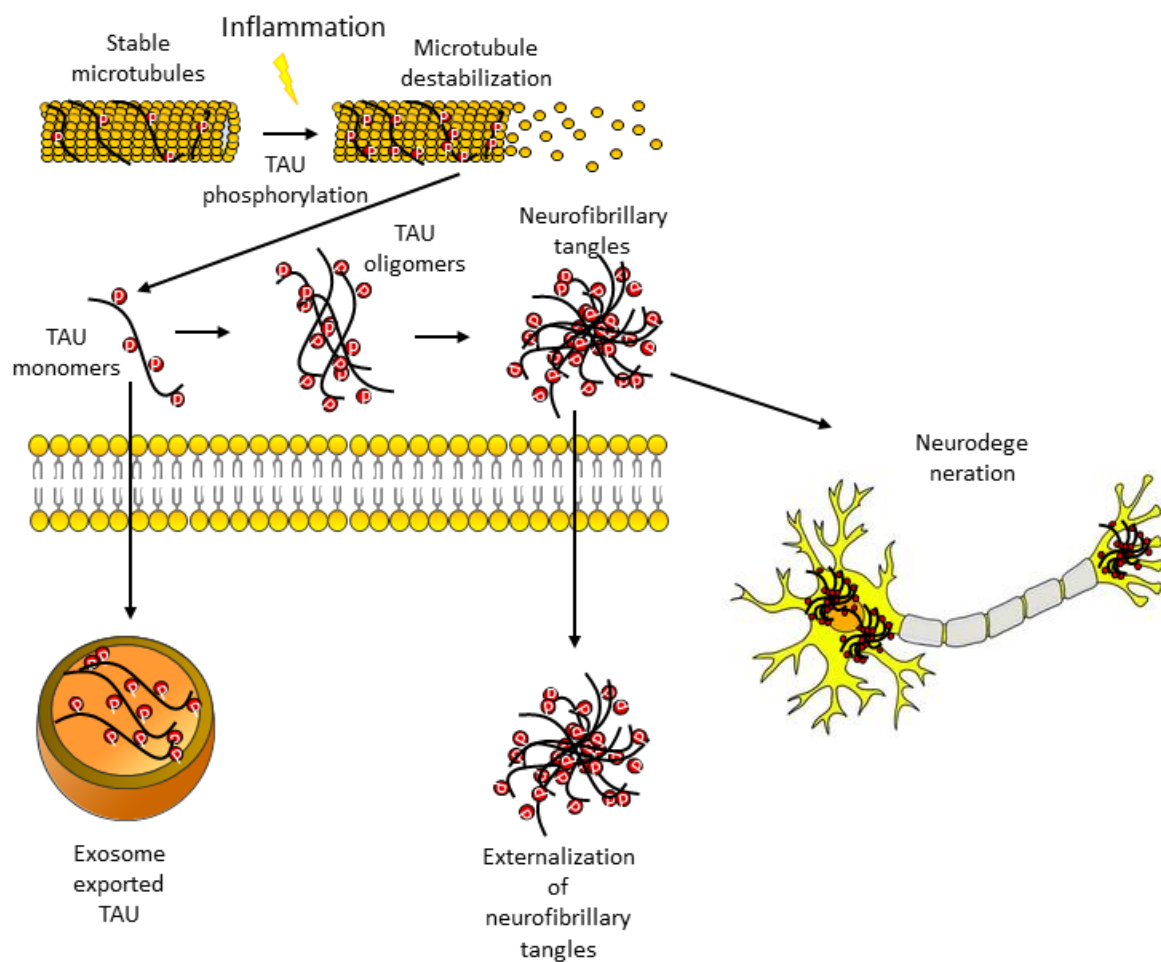


Figure 4: Progression of TAU pathology.

TAU acts as a microtubule stabilizer and has an important role in the regulation of intracellular trafficking. In Alzheimer's disease, however, TAU is hyperphosphorylated, being unable to exert its natural function, disassembling microtubules and aggregating in neurofibrillary tangles. TAU phosphorylation is normally caused by inflammation induced by ROS or amyloid- β . The degree of phosphorylation reflects the activity of protein kinases and phosphatases, such as cyclin-dependent-like kinase 5 (CDK5) or glycogen synthase kinase 3 β (GSK3 β). Both molecules are upregulated in Alzheimer's disease and are known to phosphorylate TAU in different sites^[37]. After being phosphorylated, TAU monomers aggregate into soluble oligomers, being later incorporated in neurofibrillary tangles, as their major component. Although TAU phosphorylation is one of the earliest stages of Alzheimer's disease, the formation of neurofibrillary tangles does not start until the late stages of the disease. The neurofibrillary tangles can be exported to the extracellular space, where they can be incorporated by other cells and thus accelerating the disease progression. Interestingly,

exosomes containing TAU were detected in the cerebrospinal fluid of patients with Alzheimer's disease. Exosomal TAU was found in a larger extent in patients with an early stage of AD. In the late stage of this disease TAU was found in greater quantities outside of the exosomes, in the extracellular lumen. The neurofibrillary tangles found in later stages of the disease are prone to bear bigger toxicity, aiding the loss of neurons and on the cognitive decay^[38]. Recent studies show that using siRNA against microtubule associated protein tau (MAPT) gene that regulates TAU expression, downregulates its production. The reduced levels of phosphorylated and normal TAU are strongly linked to a reduction of amyloid- β production and toxicity, as well as reduction of mitochondrial oxidative insults and synaptic damage to neurons^[39].

1.6 Diagnosis and treatment of Alzheimer

Since the discovery of this disorder in 1905 by Alois Alzheimer, several substances have been purposed to attenuate or revert it^[40]. However, as the disease does not present major symptoms on its early stage, there is a significant delay on its early detection resulting on a poor prognosis for the patient. In addition, there is not any method to detect Alzheimer's disease before the aggregation of amyloid plaques. So, Alzheimer treatment in its early stage is still limited. Moreover, there are no well-founded biomarkers to determine the progress or the relapse of the disease^[41].

In order to detect this disease, various techniques have been used in the past few years, which are complementary of each other. These techniques include magnetic resonance imaging (MRI), molecular positron emission tomography (PET) and single-photon emission computed tomography (SPECT). These techniques can establish a positive differential diagnosis in almost every stage of the disease, excluding its early stage. PET and SPECT can give information of the global neuronal activity, neurotransmission and the imaging of neuropathological lesions, using amyloid/tau imaging^[42]. MRI imaging has been improved with the use of nanoparticles with high contrast agents or tagged with fluorescent probes, to detect the amyloid plaques. These nanoparticles have several advantages, such as versatility and ability to go through the blood brain barrier, due to their small size^[8].

There are various targets for the treatment of Alzheimer's disease, like the reactive oxygen species, neurotransmissions, TAU protein, amyloid- β and its precursors^[43]. The targeting of oxidative stress can be used to decrease the production levels of amyloid- β protein, and TAU phosphorylation

levels. Nowadays, antioxidant therapies include the use of curcumin, lipid soluble vitamin E, and the use of metal-protein-attenuating compounds (MPACs)^[44] that decrease the interaction between proteins and ions. It is known that metal ions can have nefarious effects on the central nervous system as this disease progresses. The use of drugs such as clioquinol has shown some promising results on phase 2 clinical trials^[45].

The number of therapeutic molecules in clinic for the treatment of Alzheimer's disease is very low and there are some in clinical trials. Some of them have interesting results like memantine. This molecule is a receptor antagonist, which has been approved for the treatment of late-stage Alzheimer's disease^[46], and until now no other molecule has been approved for Alzheimer's disease treatment. Memantine promotes circuit connectivity, contributing to synapse integrity.

Currently, several molecules are being studied due to their ability to compromise the expression of amyloid- β and inhibiting the cascade that triggers cellular dysfunction^[31]. Verubecestat, for example, is a substance that can reduce amyloid- β production with satisfactory results and almost no side effects. Solanezumab, Gantenerumab and Aducanumab are monoclonal antibodies that have been tested for the reduction of amyloid- β production. Solanezumab targets and reduces soluble amyloid- β ^[47], while Gantenerumab reduces amyloid- β plaques by recruiting microglia. Aducanumab binds to parenchymal amyloid- β and reduces its soluble and insoluble forms^[48]. Another promising technique is the clearance of amyloid- β from the brain. Different drugs have been used to decrease neuroinflammation, like ALZT-OP1, which is a combination of cromolyn sodium and ibuprofen^[49].

Drugs that target neurotransmitters such as donepezil, rivastigmine and galantamine are also used for the treatment of Alzheimer's disease. These particular molecules are acetylcholinesterase inhibitors. These molecules have been derivatized to improve their efficacy and to reduce their toxicity^[50].

More recently, a new approach is being developed to overcome Alzheimer's disease: the use of miRNA. This molecule, however, needs a carrier to reach the brain. Cationic lipid nanoparticles, gold nanoparticles, hydrogels, carbon-based carriers, mesoporous silica nanoparticles and magnetic nanoparticles are some of the most interesting nanocarriers to deliver miRNAs to the brain. The last ones showed interesting results since they can be guided by an external magnetic field to a precise location for the molecule delivery^[51].

1.7 Blood brain barrier – the mediator of molecule internalization into the brain

The brain has peculiar characteristics that make the treatment of diseases associated with it especially difficult. The blood brain barrier is the first and the principal barrier that prevents the entry of molecules into the brain^[52]. While this barrier is advantageous in most cases, it poses a great challenge when the delivery of therapeutical molecules is needed. A significant number of drugs designed to treat brain disorders, or minimize their symptoms have difficulties to bypass the blood brain barrier. So, the development of a carrier that can bypass this barrier, delivering the drug *in situ*, is of utmost importance.

There are several techniques that can be used to maximize drug delivery into the brain. These include chemical delivery systems, such as lipid-mediated systems; biological delivery systems, in which pharmaceuticals are re-engineered to cross the blood brain barrier. It is possible to induce a transient disruption the blood brain barrier, causing an hypotonic environment around endothelial cells, leading to their shrinkage, and thus opening the tight junctions. The use of molecules that transport the drug directly to the brain, passing the blood brain barrier, without disrupting it, is also becoming a predominant technique, since it is a less invasive technique.

1.8 Blood brain barrier intake pathways

The biggest challenge for the neurodegenerative diseases therapy is the difficulty that therapeutic molecules have to reach the brain. The blood brain barrier separates the blood circulation from the brain parenchyma^[52]. This barrier is a strong physical barrier due to the presence of tight junctions, but it is also permeable and highly, selective. In order to accomplish these requirements, the blood brain barrier has control mechanisms for the interchange of molecules between brain's parenchyma and blood capillaries. This interchange it is highly dependent on molecule size, charge, and specific active groups^[53].

Endothelial cells present on the blood brain barrier have two membranes: a luminal membrane in the side of the blood and the abluminal membrane at the parenchyma's side. In the

abluminal membrane the endothelial cells are supported by astrocytes and pericytes which express enzymes that inactivate harmful substances that are able to cross the blood brain barrier^[54].

The molecules that can bypass the blood brain barrier can be divided in 4 groups: hydrophilic molecules, ions and low molecular mass solutes; lipophilic molecules; charged molecules and other molecules such as insulin, leptin, transferrins and low-density lipoproteins.

Hydrophilic molecules, ions and low molecular mass solutes cross the blood brain barrier through paracellular transport. This transport is controlled by tight junctions and it is highly dependent on the solute and ion concentration. Lipophilic molecules can cross the blood brain barrier using the transcellular pathway. These molecules are diffused through the lipid membranes of the endothelium in an energy or non-energy dependent way. Charged molecules interact with the negatively charged endothelium cells, which internalized them by adsorptive mediated transcytosis. Other molecules such as insulin, leptin, transferrins and low-density lipoproteins can also be internalized by receptor-mediated transcytosis. This process is however dependent on the temperature and the receptor-ligand saturation.^{[55],[53]}

1.9 Nanoparticles: advantages and utility

Since the discovery of nanoparticles, they have been used in almost every field of knowledge, from medicine to industry^{[56],[57]}. In plastic industry, nanoparticles are used to reinforce the plastics; in the food industry nanoparticles are used to improve aliments' texture, flavor, enhance the absorption of nutrients and improved packing, and security of food products^[58]. The nanoparticles can also be used in water waste treatment. ^[59] As to their biomedical applications nanoparticles stand out as one of the most promising systems for the delivery of pharmaceuticals that otherwise would cause cytotoxicity, be eliminated, or have a low bioavailability.

Nanoparticles have unique and interesting characteristics. Their size ranging from 1 nm to 200 nm and high surface area give them properties that widely differ from the macroscale objects^[60]. The nanoparticles' properties depend on the type of material used, as well as the preparation method along with temperature and pH^{[61],[62]}. As the safety of these nanoparticles is widely dependent in their charge, size and shape, the design approach to develop these systems has to be perfected in order to optimize these factors^[63].

As mentioned, nanoparticles have interesting properties for drug delivery, but its safety has been questioned since their discovery^{[64]-[66]}. The studies of their impact in human health and in the environment are in an early stage, but they point out that the accumulation of these particles, particularly metal nanoparticles^[67] in kidney and liver vary can be harmful^[68]. Moreover, studies indicate that these particles can be harmful to some animal species, affecting the whole food chains due to bioaccumulation^{[69];[70]}. Therefore, the production of non-cytotoxic nanoparticles has become one of the major challenges for nanotechnology, with liposomes being one of the most biocompatible systems already used in therapy^[71].

1.9.1 Liposomes

Nanotechnology is present in many therapies for neurological diseases. There are a wide number of systems that have been developed to treat or slow down these diseases^[72]. One commonly used system for the treatment of neurological diseases are liposomes, showing interesting results in Parkinson^[73] and Alzheimer's^[74].

These nanocarriers can be very versatile as their lipid composition can widely vary. They can be functionalized with a wide range of molecules, that can target the desired cells or protect them from the immune system. The conditions of production of these liposomes can be tuned in order to modify their properties.

Liposomes can be characterized in 4 major groups: small unilamellar vesicles (SUVs), large unilamellar vesicles (LUVs), multivesicular vesicles (MVs) and multilamellar vesicles (MLVs). Depending on the strategy for the cargo release, liposomes can be characterized as pH sensitive, that destabilize at a certain environmental pH; temperature sensitive, that release their cargo when, by an internal or external stimulus, the temperature rises, or drops below the body's normal temperature; and immunoliposomes, that are modified with antibodies for specific targeting^[71].

The composition of liposomes can be similar to biological membranes. Therefore, they will not bioaccumulate or be eliminated by the organism. Liposomes are often characterized by their size, superficial charge, lipid composition and functionalization^[75]. The fact that these characteristics can be tunable in order to obtain the desired liposomal properties, makes them extremely versatile nanocarriers. When adding the fact that liposomes can carry both hydrophilic and lipophilic molecules,

often having excellent encapsulation efficiencies and loading a large quantity of molecules in just one liposome, it becomes evident that these systems are the most common and well-researched nanocarriers for the delivery of bioactive molecules^[75].

1.10 Nanocarriers used in the treatment of Alzheimer's disease

Currently, molecules to target Alzheimer's hallmarks are being delivered by nanocarriers. Due to the specificities of the blood brain barrier, several nanocarriers have been developed, as described in table 1.

Organic nanoparticles are some of the most promising carriers due to their higher flexibility and easiness to produce. Moreover, tailoring organic compounds is infinite^[76]. Some organic nanoparticles are particularly interesting such as liposomes and exosomes, due to their lipid composition similar to the plasma membrane.

Table 1: Nanocarriers used in the treatment of Alzheimer's disease and the encapsulated molecules.

	Nanocarriers	Molecules	Ref.
	Polymeric nanoparticle		
Inorganic nanoparticles	Gold nanoparticles		
	Silica nanoparticles		[77], [78], [79],
Organic nanoparticles	Liposomes	Curcumin, quercetin, piperine, cyclodextrins;	[80], [81], [82],
	Chitosan nanoparticles	Bace1 siRNA; A β binding peptides	[83], [84], [85],
	Albumin nanoparticles		[86]
	Solid lipid nanoparticles		
	Exosomes		

All these nanocarrier are capable to pass the blood brain barrier. Once inside the brain, they face another challenge; avoid the recognition by microglia. Microglia behaves like other immune cells in the body, recognizing, targeting and eliminating strange molecules. Thus, when thinking about the delivery of a drug, it is essential to take in account these cells' function.

1.11 Curcumin properties and effects in Alzheimer's disease treatment

Curcumin is a well-known compound derived from the rhizomes of turmeric (*Curcuma longa*), with well-studied antioxidant properties. This is a widely used Indian spice, that is usually present in curry and mustard. It has been used for thousands of years as a traditional medicine^{[87],[88]} for the treatment of arthritis or as an antiseptic for cuts, burns and bruises. In Ayurvedic culture this compound can be used to treat respiratory conditions, liver disorders, diabetic wounds, anorexia and cough^[89].

Curcumin is extremely sensitive to light, but stable at high temperature that can reach 250°C.^[90] Curcumin can be extracted from an herb from the *Zingiberaceae* family, which has a yellow pigmentation. There are three major components present in turmeric: 77% of curcumin, 17% of dimethoxy curcumin and 3% of bis-demethoxy curcumin.^[91] Curcumin is a relatively safe compound, not showing any toxicity, or side effects in its administration. For example, in a study conducted by Mahmood *et al.*, an oral administration of 12g/day has not shown any significant side effects^[92].

The effects of curcumin in neurodegenerative diseases have been highly studied for the past few years, with promising results, namely in the treatment of Alzheimer's disease. Fusheng *et al* demonstrated that the presence curcumin inhibit amyloid- β oligomers formation in neuroblastoma cells leading to an higher cell viability.^[93] Moreover, its anti-inflammatory properties, due to its enol form, most predominant at alkaline pH, acts as a ion chelator in positively charged metal cations, reducing neuroinflammation associated with this disease.^[92]

Despite its interesting properties, this hydrophobic polyphenol, has some major setbacks regarding its administration and bioavailability. This molecule has low water solubility, low stability, and, since it is not targeted for specific cells, can be rapidly absorbed and metabolized in a non-specific way. Moreover, curcumin in its free form is poorly absorbed in the gastrointestinal tract^[94]. In order to overcome these problems, drug delivery systems like nanocarriers have been developed^[92].

According to the literature, curcumin has been encapsulated in several nanocarriers like polymeric micelles^{[95]-[97]}, protein or peptide carriers^[98] and cyclodextrins^{[96],[97]}. From all these carriers, liposomes stand out, since they are biocompatible, biodegradable, highly stable, non-cytotoxic and can have a sustained drug release.

Liposomes can deliver the drug in the targeted location increasing the efficiency of the therapy. After the release of the molecule, liposomes are majorly accumulated in the liver (approximately 90%), and eliminated from the organism.^[99]

1.12 Gene silencing therapy

Since the discovery of gene silencing therapy, and the first authorized gene transfer study in 1989^[100], its definition has changed. Initially, the definition of gene therapy would only comprise the replacement of a defective gene for one healthy one. Nowadays, this term can be utilized for any treatment that uses any kind of nucleic acid to treat or prevent any disease^[101]. This includes replacing, correcting or silencing a mutated gene, gene marking or gene editing or reprogramming^[102].

The administration of gene silencing therapy is normally done using viral carriers. Viral carriers are the most used vectors for this approach due to their capacity to penetrate the targeted cell, high efficiency and long-term expression. Although, they have serious downsides mainly their cytotoxicity, and genotoxicity^[102]. So, non-viral carriers like liposomes have been developed, which are less cytotoxic and still efficient gene delivery nanocarriers.

1.12.1 RNA interference therapy

In the past few years, RNA interference has become a promising therapy. With the disclosure of the human genomic data, and the possibility to design oligonucleotide agents based in mRNA transcripts, every gene can be downregulated using the RNAi mechanism. These therapeutic oligonucleotides can be divided in several categories, due to their mechanism of action. The most important ones include: Antisense; aptamers; splice correcting oligonucleotides; siRNA; miRNA mimics and antagonists; immunomodulating agents and decoys.^[103]

The use of siRNA for silencing genes responsible for the overexpression of proteins responsible for the initialization or progression of some diseases is emerging as one of the most promising therapies. The versatility, specificity for the targeted site in the messenger RNA (mRNA), and the efficient knockdown of the gene contribute for the rising popularity of this technique^[104].

Small interfering RNA (siRNA) is a class of small (20 to 25 base pairs in length), double stranded RNA. siRNA interferes with the expression of genes with complementary nucleotide sequences degrading the mRNA after transcription. This molecule can be used for the treatment of various diseases, from viral infections to cancer and neurodegenerative diseases. The systemic delivery of siRNA is a difficult task, due to its unfavorable pharmacokinetics and biodistribution profiles. Naked siRNA will not only be accumulated in the targeted cells, but also in other tissues and organs. siRNA also has poor circulation stability and is susceptible for degradation by extracellular RNases^[105]. Moreover, as the plasma membrane has a selective permeability, siRNA molecules will not be able to diffuse through this barrier due to its highly negative charge^[106]. In order to overcome the referred issues various strategies have been used in the past few years, including the modification of siRNA, or the use of nanocarriers^[107]. Viral nanoparticles have an effective delivery *in vitro* and *in vivo*, but their low selectivity and cytotoxicity are a setback. So, lipid nanocarriers are the most promising transporters for siRNA delivery; particularly due to the ability to functionalize them to target a specific type of cell, as well as low toxicity.

1.13 Exosome composition and formation

Exosomes are lipid nanocarriers composed by a bilayer that can encapsulate from proteins to nucleic acids^[108]. The composition of its lipid bilayer is highly similar to the cell's membrane (**figure 5**).

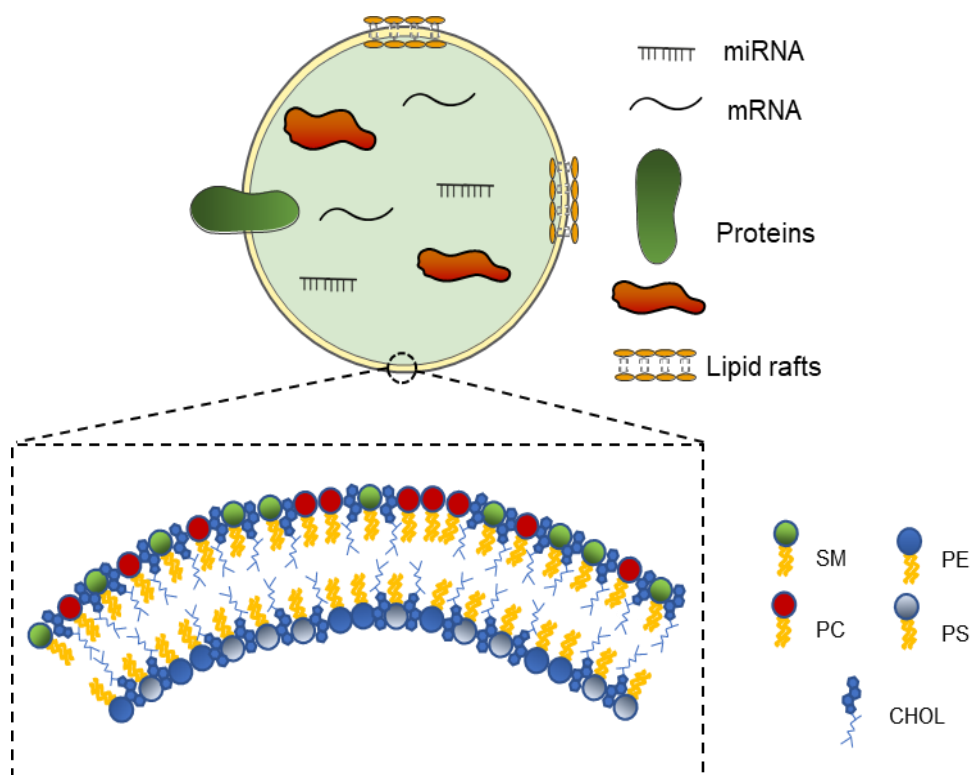


Figure 5: Exosome components and lipidic constitution: cholesterol (CHOL); sphingomyelin (SM); phosphatidylcholine (PC); phosphatidylserine (PS) and phosphatidylenositol (PE).

Exosomes are a homogenous population of 20-150 nm nanovesicles formed from endosomes originated from invaginations of the plasma membrane^[109]. Exosomes go through 4 important stages in their formation: (i) initiation, (ii) endocytosis, (iii) multivesicular bodies formation and (iv) exosome secretion. At the final stage exosomes with encapsulated molecules are exported from their original cells^[110]. The exosomal content and membrane lipid composition depends on the parental cell.

1.13.1 Therapeutic administration of exosomes

Exosomes biodistribution is determined by the administration route, dose and cellular origin. The recognition of exosomes by the cells is still poorly understood. It is reported that adhesion^[111], free floating^[112] and antigen-presentation^[113] are the most common recognition mechanisms. Similarly, the

internalization of exosomes into the target cells is not fully understood^[114]. However, some internalization routes, like soluble and juxtacrine signaling, fusion, phagocytosis, micropinocytosis, receptor and raft mediated endocytosis stand out as the major internalization routes^[112].

1.14 Exosome-like nanoparticles

Exosome-like particles can be divided in two distinct categories. The first one, natural exosome-like nanoparticles and the second one synthetically produced exosome-like nanoparticles. On the first group it is possible to highlight the exosome extracted from plants and fruit, which have a similar composition of mammalian exosomes. These exosomes are mostly extracted from grape, grapefruit (GELNs)^[115], grapefruit-derived exosome-like nanoparticles (GDNs)^[116], exosome-like nanoparticles isolated from coconut water^[117], *Citrus limon* derived nanoparticles^[118], ginger and carrot nanoparticles^[119]. All the systems from this group have characteristics similar to cell membrane constituent or to human exosomes. Their size ranges from 50 nm to approximately 150 nm. A major drawback of natural exosome is their long and expensive isolation and purification. Synthetic exosomes can be prepared by serial extrusion through a polycarbonate membrane of different cell lines. Lunavat *et al.* demonstrated that by serial extrusion through 10 μm , 5 μm and 1 μm polycarbonate membrane filters of NIH3T3 cells they can generate exosome-like nanoparticles with approximately 150 nm. These nanoparticles can encapsulate siRNA, target and downregulate the major regulator in cell growth, c-Myc, in λ 820 cells for cancer therapy^[120]. This serial extrusion technique was also replicated by Jang *et al.*, that resulted in the development of exosome-like nanoparticles from human U937 monocytic cell line, for delivery of chemotherapeutics such as doxorubicin for malignant tumors^[121]. Following the same principle, Bryniarski *et al.* produced exosome-like particles from CD8⁺ T cells, that can suppress Ag-specific CS-effector T cells These particles were also used by the same group to encapsulate and deliver siRNA^[122]

One example of a bottom up approach in developing synthetic exosome-like nanoparticles can be found in the work done by Chen *et al.* They developed exosome-like silica nanoparticles composed of hexadecyltrimethylammonium bromide (CTAB), ammonia, decane, dimethylhexadecylamine (DMHA) and silica have also been produced^[123]. Although they have low cytotoxicity and have a size similar to exosomes (140 nm) they do not mimic exosomes composition. Thus, the production of a

system that has both the lipid constitution and properties of exosomes, without the long processes of extraction and isolation is yet lacking.

1.15 Objective

Since the discovery of the antioxidant effects of curcumin, some therapies have been proposed for the delivery of this molecule to the brain. Exosomes, as naturally occurring vesicles linked with the transport of TAU and amyloid- β , are interesting carriers that have been proposed for Alzheimer's disease therapy directly targeting the brain. These nanocarriers, as they are naturally occurring vesicles, do not induce any cytotoxicity. They can also be easily incorporated by cells. Exosome-like liposomes, which overcome some limitations associated with exosomes, are emerging as promising carriers of bioactive molecules. Yet, there are no reports of such a exosomal-like system which can incorporate curcumin and deliver it to the brain. Furthermore, the encapsulation of nucleic acids in these vesicles is yet in its early steps. The dual delivery of curcumin and therapeutic nucleic acids would therefore be a major breakthrough for Alzheimer's disease potential new treatments.

So, in order to alleviate the symptoms of Alzheimer's a treatment with curcumin and siRNA against TAU would target the hallmarks of the disease and slow it's progression.

Our group developed a new type of exosome-like nanoparticles, constituted by lipids that mimic natural exosome composition. The main goal of this work was to optimize loading of both curcumin and siRNA in these exosome-like liposomes and evaluate encapsulation efficiency, as well as cytotoxicity and bioactivity using *in vitro* mammalian cell culture, namely to measure the neuroprotective effects of curcumin.

2 Materials and Methods

For the encapsulation of siRNA and curcumin, two formulations of exosome-like liposomes were tested. The first one, the most similar to naturally occurring exosomes, contains cholesterol, DPPC, sphingomyelin and finally PEG-ceramide, that is not found in the natural composition of exosomes but is needed to shield the exosome-like liposomes from an immune response^[124]. An additional formulation was prepared, with slight variations such as inclusion of DODAP, essentially to

give the exosome-like liposomes a positive surface charge, to facilitate electrostatic encapsulation of the siRNA.

2.1 Materials

Cholesterol, sphingomyelin, Dipalmitoylphosphatidylcholine (DPPC), 1,2-dioleoyl-3-dimethylammonium-propane (DODAP) and N-palmitoyl-sphingosine-1-{succinyl[methoxy(polyethylene glycol)2000]} (PEG ceramide) were purchased from Avanti Polar Lipids (Alabaster, AL). The RiboGreen kit was acquired from Invitrogen (Eugene, OR). Fetal bovine serum (FBS), Ham's F-12 medium and Penicillin/Streptomycin were purchased from Biochrom GmbH (Berlin, Germany). Dulbecco's Modified Eagle's Medium- high glucose (DMEM), 7-Hydroxy-3H-phenoxazin-3-one-10-oxide sodium salt (resazurin), 4-(2-Hydroxyethyl)piperazine-1-ethanesulfonic acid, N-(2-Hydroxyethyl) piperazine-N'-(2-ethanesulfonic acid) (HEPES buffer), 2-(N-Morpholino)ethanesulfonic acid, 4-Morpholineethanesulfonic acid (MES buffer), citric acid, sodium citrate, trypan blue and *Curcuma longa* were acquired from Sigma-Aldrich (St. Louis, MI). 4',6-Diamidino-2'-phenylindole dihydrochloride (DAPI) was obtained from Acros Organics/Thermo Fisher Scientific (Waltham, MA). Infinity Cholesterol® was acquired from Thermo Fisher Scientific (Waltham, MA). siRNA targeting TAU (5' rCrArUrCrCrArUrCrArUrArArCrCrArGrGrATT') was purchased from Integrated DNA Technologies (Leuven, Belgium). Absolute ethanol was acquired from Merck (Darmstadt, Germany).

2.2 Lipid solutions

The different lipid concentrations were prepared by adding the necessary lipid mass to 1 ml of absolute ethanol or chloroform in the case of DODAP (table 2). The solutions were dissolved at a temperature above 60 °C, followed by vigorous vortexing. The lipid solutions were then stored at -20 °C until use.

2.3 Curcumin solution

A 10 mM solution of curcumin was prepared by solubilizing 3.7 mg of *Curcuma longa* in 1 ml of absolute ethanol. Due to curcumin photosensitivity ^[125] the solution was prepared in the dark, and stored at -20°C, protected from light.

2.4 Buffers

HEPES buffer preparation (pH 7.4)

Briefly, 4.77g of HEPES and 8.474g of NaCl were dissolved into 1 L of ultrapure water to obtain a final concentration of 20 mM of HEPES and 14.50 mM of NaCl. The pH was adjusted to 7.4 using a solution of NaOH, 20 mM. The solution was then filtered through a 0.20 μm pore diameter filter, and stored at 4 ° C.

Citrate buffer preparation (pH 3)

For this buffer, citric acid and sodium citrate (0.33 g and 0.09 g respectively) were weighed. These compounds were dissolved in 200 ml of water. The pH of this solution was not corrected, as the solution already had pH = 3.00.

2.5 Exosome-like liposome preparation

All exosome-like liposomes were prepared by ethanolic injection. This technique consists on the injection of the lipids dissolved in ethanol, into an aqueous solution, such as water or an aqueous buffer.

Table 2: Concentration of the stock solution and percentage of the various lipids used in the preparation of the exosome-like liposomes.

Lipid	Concentration (mM)	Lipid percentage in the formulation (%)
Cholesterol	40	0.50
DPPC	30	0.30
Sphingomyelin	30	0.15
PEG-ceramide	20	0.05

Briefly, 400 μ l of the lipid solution (described in table2) were added, dropwise with a pipette tip, under vigorous vortexing, in aliquots of 60 μ l, alternating cycles of injection of these aliquots and to a 600 μ l solution with HEPES buffer.

2.6 Preparation of exosome-like liposomes with DODAP

DODAP has a positive charge at acidic pH and a neutral charge at pH=7.4; so citrate buffer at pH=3 was used to prepare these exosome-like liposomes. The preparation of this formulation was performed similarly to the one described at section 1. For these exosome-like liposomes, a film was made, to which the remaining lipids (162.5 μ l of cholesterol, 65 μ l of sphingomyelin and 32.5 μ l of PEG-ceramide) were later added. The lipid film was made by pipetting 84.2 μ l of a DODAP solution and 86.7 μ l of a DPPC dissolved in chloroform at a concentration of 40 mM and 30 mM, respectively. The solutions were added to a test tube, and the chloroform evaporated on a rotary evaporator. The remaining lipids were added to this film, and this solution is injected in 60 μ l aliquots into 400 μ l of citrate buffer with the siRNA alternating between injection under vortexing and incubation in a bath at 60° C, above the phase transition temperature.

2.6.1 Separation of the encapsulated and free fractions

Two steps were used to separate the encapsulated siRNA in the exosome-like liposomes from the free, unencapsulated siRNA: i) purification of the exosome-like liposomes in a molecular exclusion column, and ii) the separation of the two fractions using amicons® with a pore size of 100 nm. This process is essential to enable further quantification of the encapsulated siRNA. This step guarantees that the free siRNA cannot interfere with the quantification of the encapsulated siRNA.

2.6.1.1 Exosome-like liposome purification in a molecular exclusion column

Exosome-like liposome purification was realized so that any unencapsulated siRNA or curcumin does not interfere in further quantification of the encapsulated siRNA and curcumin. This process consisted in the passage of aliquots of 200 μ l of the exosome-like liposomes with HEPES buffer through a molecular exclusion column, separating the exosome-like liposomes and the free curcumin and siRNA altering the concentration of the exosome-like liposomes. A subsequent lipid quantification was necessary, by quantifying the cholesterol present in the samples to determine the new concentration of exosome-like liposomes.

2.6.1.2 Separation of the encapsulated and free fractions of siRNA using amicons®

This procedure was performed by subjecting 500 μ l of the previously prepared exosome-like liposomes to centrifugation for 15 min at 14000 rpm and 4 ° C (temperature at which the RNases do not act). The centrifugation was performed in an amicon® with 100 nm pore PES membrane. Both portions (encapsulated and free siRNA) were immediately stored on ice, and the measurement of the free siRNA was performed immediately. After each use the amicon® was washed and centrifuged at 14000 rpm for 15 min with absolute ethanol (1x) and ultrapure water (2x) in order to remove any contamination at a later time.

2.7 Size and polydispersity determination by Dynamic light scattering (DLS)

This technique consists in the measurement of the scattered light from small particles. This process can give information about the particle's proportion and their state of motion. It consists in measuring the diffusivity of the particles, when undergoing Brownian motion^[126].

For spherical particles, the Stokes-Einstein equation can be used to establish the relationship between the diffusion coefficient D_T and the hydrodynamic diameter of the particles:

$$D_T = \frac{K_B T}{3\pi\mu D}$$

Equation 1: Stokes-Einstein equation where K_B is the Boltzmann constant, T is the absolute temperature, D is the particle's hydrodynamic diameter and μ is the dynamic viscosity of the medium

This hydrodynamic diameter is a theoretical diameter of a sphere that diffuses light in the same way as the particle that is being measured.

The scattering light fluctuates randomly, with the Brownian motion of the particles. Small particles move faster than large ones, making this random fluctuation of the scattering light also faster^[127].

The particles in the measured sample have a certain degree of heterogeneity. The polydispersity index (PDI) is used to determine the uniformity of the sample, in terms of the particle's size. The sample is monodisperse if the PDI is below 0.1 and polydisperse for higher values. There are many factors that can affect the polydispersity of one sample such as the heterogeneity of the particles, their aggregation, or their contamination. High polydispersity values can lead to unreliable results, far from the real size of the particles^[126].

Briefly, an aliquot of 10 μl of each exosome-like liposome sample was diluted in 990 μl of HEPES buffer. This solution was placed in a polystyrene cuvette and the size and PDI were measured, with an attenuator between 6 and 9 and a count rate always superior to 150 counts.

2.8 Surface charge measurement by Electrophoretic light scattering (ELS)

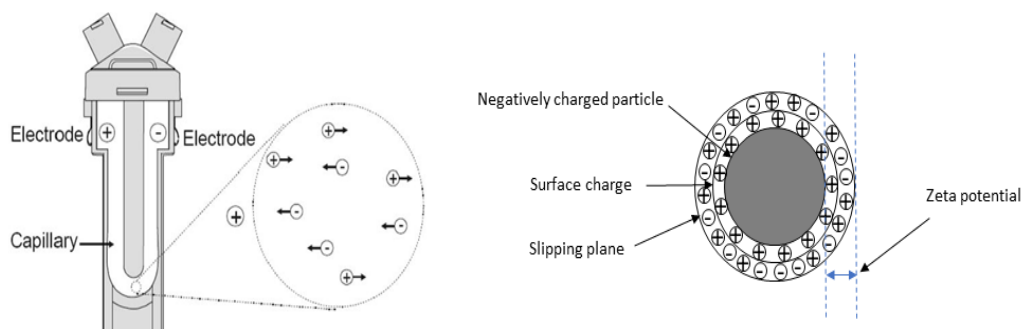


Figure 6: Schematic representation of a dip cell. Adapted from^[151]

This technique is based on the electrophoretic principles. When a solution is introduced into a cell that has two electrodes, and an electrical field is applied to the electrodes, the particles that have a net charge, will migrate towards the oppositely charge electrode. This migration has a certain velocity, known as the mobility of the particles, that is related to their zeta potential.

This technique is used to measure particle charge in solution. It does not measure only the outer layer of the particle, but also its solvation layer. The charge felt between these two layers is called zeta potential. This has a wide range of implications, being the most important one that the real charge of the particle can be mitigated by the solvent.

For this measurement, an aliquot of 800 μl of the solution prepared for the DLS analysis was placed in the zeta cuvette.

2.9 Exosome-like liposome lipid concentration quantification

Exosome-like liposomes purification in the exclusion column changes the initial lipid concentration. Moreover, the use of amicons® to separate the free fraction from the encapsulated siRNA also alters the concentration of the exosome-like liposomes. Lipid quantification is necessary to calculate the efficiency of siRNA encapsulation, that is expressed relative to the lipid concentration in solution. The lipid quantification process in the sample consists on the quantification of cholesterol. This quantification was carried out by the Infinity™ cholesterol method, and the result was stipulated to be the total lipid concentration. The measurements were done according to the

manufacturer's instructions. The comparison of the samples with the standards with known concentrations, enables the precise calculus of the lipid concentration in the samples. Dilution factors, as well as the percentage of cholesterol in relation to the total lipid were considered.

2.10 Lysis of the exosome-like liposomes for the quantification of encapsulated siRNA

In order to determine which detergent would cause greater destabilization of the exosome-like liposomes, for the better release of siRNA, four detergents were tested: C₁₂E₈, Triton 10X, Tween 20 and Tween 80. The evaluation of the liposomal destabilization caused by these four compounds was performed by DLS. Treatment of the exosome-like liposomes with the detergents consisted on the mixture of 6 µl of detergent to 1 µl of exosome-like liposomes in 93 µl of ultrapure water. This solution is subsequently heated to 60 ° C, and vortexed vigorously. This step allows a better action of the detergent on the destabilization of the exosome-like liposomes. The solutions were immediately stored on ice to prevent degradation of the siRNA, and the size and PDI of these samples are then measured. Finally, the concentration of siRNA released by the exosome-like liposomes was measured.

2.11 Encapsulated siRNA quantification

Encapsulated siRNA quantification was performed using RiboGreen®, and the fluorescence measurement was obtained for each sample using the chosen detergent: C₁₂E₈. Treatment of the exosome-like liposomes with this compound was reported in the previous step. As soon as the samples reach room temperature, they were transferred to a 96-well fluorescence plate. 100 µl of RiboGreen® 200x was added immediately. After a 5 min incubation protected from light, the fluorescence of the samples was measured at $\lambda_{exc}=485\text{nm}$ and $\lambda_{em}=538\text{ nm}$. The concentration of siRNA in each sample was obtained by the calibration curve (**figure 7**) performed previously.

The calibration curve represents a linear relationship between the fluorescence intensity of the samples and their siRNA concentration. Thus, through the equation it is possible to know the concentration of siRNA present in the several samples.

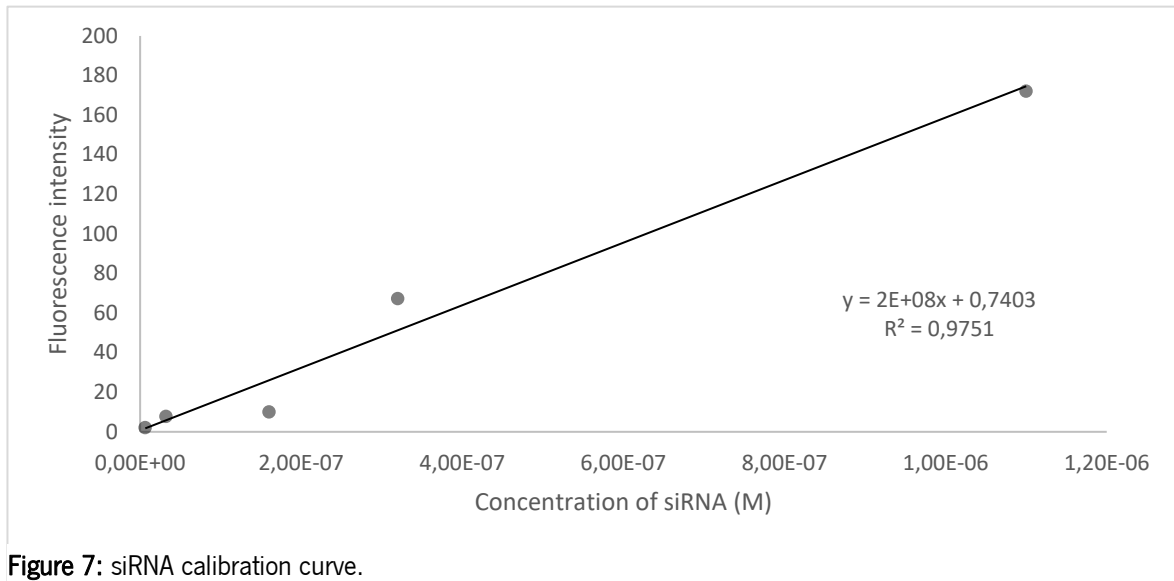


Figure 7: siRNA calibration curve.

The number of moles of lipid and siRNA on each formulation was calculated. The experimental and theoretical relationship between the number of moles of siRNA and lipid present in the exosome-like liposomes was calculated by the following equation:

$$\frac{\text{n}^\circ \text{ of moles of siRNA}}{\text{lipid n}^\circ \text{ of moles in solution}}$$

Equation 2: Relationship between the number of moles of siRNA and the number of moles of the lipid in solution

The percentage of siRNA encapsulated in the exosome-like liposomes. is obtained by the following equation:

$$\%EE = \frac{\text{relation between the experimental siRNA and lipid n}^\circ \text{ moles}}{\text{relation between the teorical siRNA and lipid n}^\circ \text{ moles}} \times 100$$

Equation 3: Efficiency of encapsulation of siRNA in the exosome-like liposomes. After the calculation of the theoretical and experimental percentage of siRNA, we can calculate the percentage of siRNA encapsulated in the exosome-like liposomes by dividing the experimental value by the theoretical value of siRNA.

2.11.1 Quantification of siRNA encapsulation by electrophoresis

To confirm the efficiency of encapsulation of siRNA obtained by the fluorimetric method, using the RiboGreen® probe, an electrophoresis was performed, in the same conditions, i.e. using the same concentration of lipid for each sample. Thus, it is possible to obtain a qualitative analysis of the siRNA content in the exosome-like liposomes.

To avoid the loss of siRNA, the percentage of agarose in the gel was increased from 1% to 2%. Thus, 2 g of agarose were added to 100 ml of 1x TAE buffer. This solution was subsequently heated to solubilize the agarose. Then, 5 µl of MidoriGreen, a fluorescent probe that binds to nucleic acids, was added to the gel, allowing the visualization of the siRNA bands. After the polymerization, the samples were pipetted into the wells along with 6X LB. The samples were subjected to a constant voltage of 50V for 15min. A low voltage was used because a raise in temperature could damage siRNA.

2.12 Curcumin encapsulation in the samples

Two lipid formulations with and without DODAP were used to evaluate curcumin encapsulation efficiency. For that, an ethanolic injection method was used where curcumin was added to the lipids. A 10 mM ethanolic curcumin solution was added to the lipids, reaching 10% of the total volume of the lipid solution. This solution was heated to 60°C and injected dropwise, under high vortexing. Two different buffers were used for each formulation. 5 µl of the solution was added to citrate buffer for DODAP-containing exosome-like liposomes. Similarly, 5 µl of the solution was added to HEPES buffer for exosome-like liposomes without DODAP.

Due to the fact that curcumin is highly hydrophobic, it should be encapsulated in the exosome-like liposomes upon the ethanolic injection. After the exosome-like liposomes were formed, a 200µl aliquot of each formulation was withdrawn and passed through the exclusion column in order to remove any free curcumin in solution.

Six standards with rising concentrations of curcumin, and the same lipid concentration were also prepared. These were incubated in a Thermoblock at 60°C for 1 h and were then pipetted to a 96 well plate. The samples absorbance was measured at $\lambda_{exc}=420$ nm and $\lambda_{em}=520$ nm.

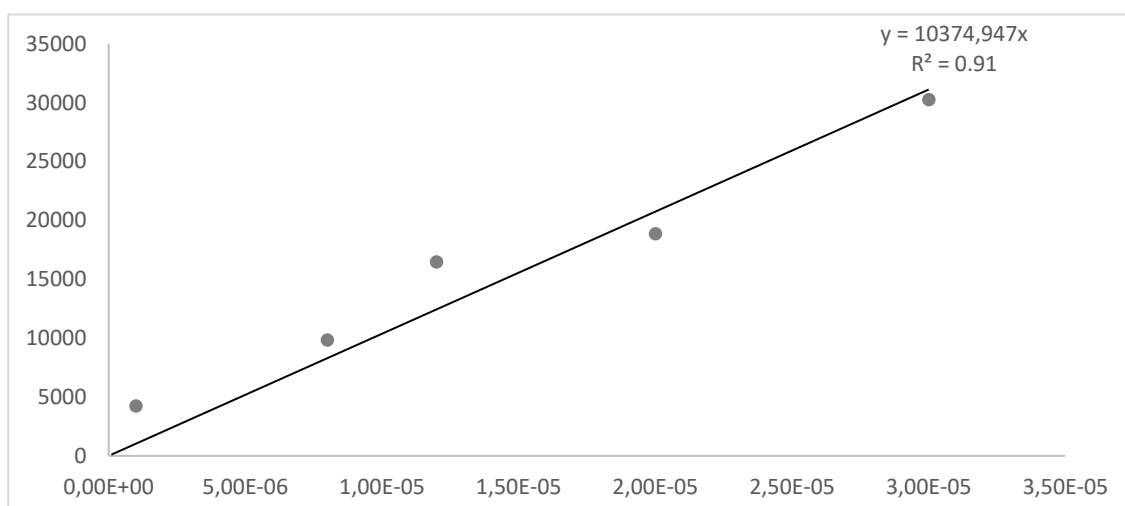


Figure 8:Curcumin calibration curve.

After these procedures, the intrinsic fluorescence of curcumin was measured in both purified and unpurified exosome-like liposomes ($\lambda_{exc}=420$ nm e $\lambda_{em}=520$ nm). This way we can guarantee that the fluorescence obtained was only due to the curcumin and not due to a greater lipid concentration.

2.13 Co-encapsulation of siRNA and curcumin in exosome-like liposomes containing DODAP

The exosome-like liposomes were prepared by initially making a lipid film with 84.2 μ l of DODAP and 86.7 μ l of DPPC. Cholesterol, sphingomyelin, PEG ceramide and curcumin at the percentage of 10% of the total volume of the solution, all dissolved in absolute ethanol, were added to this film. This lipid solution was pipetted dropwise and under strong vortexing, in the citrate buffer with 0.04 μ mol of siRNA, above the melting temperature (MT).

2.14 Curcumin encapsulation efficiency determination

The curcumin encapsulated in the exosome-like liposomes was quantified with a similar procedure as the one used for siRNA. For the quantification of curcumin, its fluorescence was used instead of a probe, as done in the siRNA assay. The value of the percentage of encapsulated curcumin was obtained by comparing the concentration of curcumin in exosome-like liposomes without

purification in the molecular exclusion column and the concentration of purified ones. The equation 4 explains the relation between these two variables:

$$EE\% = \frac{[\text{curcumin}]_P}{[\text{curcumin}]_T} \times 100$$

Equation 4: Encapsulation efficiency of curcumin. The fluorescence of the purified exosome-like liposomes $[\text{curcumin}]_P$ is divided by the fluorescence of exosome-like liposomes without purifying $[\text{curcumin}]_T$, after the utilization of a calibration curve with increasing concentrations of curcumin incubated with empty exosome-like liposomes.

2.14.1 Fourier-transform infrared spectroscopy (F-TIR)

For further corroboration of curcumin encapsulation, F-TIR was performed. Briefly, an aliquot of 10 μl of free curcumin, empty exosome-like liposomes and curcumin-loaded exosome-like liposomes was left to dry for 2 h prior to each measurement

2.15 Mammalian cell culture

Mouse embryonic cell line (L929) was used as they are widely used cells for the evaluation of nanoparticles and compound cytotoxicity. The SH-SY5Y human neuroblastoma cell line is a model for the study of oxidative stress, for systems that are proposed to reach the human brain.

Mouse fibroblastic cell line (L929) was cultivated in Dulbecco's minimal essential medium (DMEM), supplemented with 10% (v/v) of inactivated fetal bovine serum (FBS), 1% (v/v) of antibiotic/antimycotic and 1% (v/v) L-glutamine. The cells were maintained in 25 cm^2 tissue culture flasks, in an incubator with 5% CO_2 , set to 37°C. The cells were subcultured in 25 cm^2 flasks using 0.05% trypsin, before reaching confluence, in order to maintain their properties.

For the SH-SY5Y human neuroblastoma cell line, the cells were cultivated in a mixture (1:1) of Dulbecco's minimal essential medium (DMEM) and Ham's F12 nutrient Mixture, supplemented with 10% (v/v) FBS, 1% (v/v) antibiotic/antimycotic and 1% (v/v) L-glutamine. These cells were also maintained in the same conditions as described previously.

All the assays were performed under sterile conditions in a laminar flux chamber, with sterile equipment, to avoid contaminations.

2.16 Viability assessment - Resazurin assay

Resazurin reduction assay was used to test the metabolic activity of the cells. This compound can be dissolved in physiological buffers, giving the solution a deep blue coloration. Then this solution can be added to the cell culture, giving different coloration to viable cells. Cells with an active metabolism reduce the resazurin into the resorufin product which is pink and fluorescent. Then this fluorescence can be measured, and the number of viable cells can be determined, since the quantity of resorufin produced is proportional to the number of viable cells. Although resorufin quantity can be measured by a change in absorbance, this procedure is not as sensitive as the measurement of fluorescence. This technique has various advantages, which make it widely used, most of the times in detriment of tetrazolium reduction assay, or MTT and MTS assays. These advantages include its high sensibility, the fact that is relatively inexpensive, it uses an homogenous format and can be conjugated with other methods, such as measuring caspase activity, among others^[126].

L929 cell line was plated at the density of 2.73×10^4 cells/well in a 24 well plate and were left to adhere for 24h in an incubator with 5% CO₂. The medium was then removed and the exosome-like liposomes at different concentrations, in duplicates, dissolved in medium were added. A positive control containing 30% (v/v) of Dimethyl Sulfoxide (DMSO) in medium, and a negative control containing only medium, in duplicate, were also tested. After the desired incubation time (24h; 48h and 72h), exosome-like liposomes were removed and a solution of resazurin and medium (1:10) was added to the cells. After 2 h of incubation, triplicates containing 100 μ l of this medium was transferred to a 96 well fluorescence plate, and the fluorescence was measured at $\lambda_{Ex}=560$ nm; $\lambda_{Em}=590$ nm.

2.17 Cell membrane integrity - Trypan blue assay

L929 cells were plated in a 24 well plat at the density of 2.73×10^4 cells/well and were left to adhere for 8h in an incubator with 5% CO₂ and 95% air. The medium was then removed and the exosome-like liposomes, in duplicates and the positive (30% (v/v) DMSO) and negative (only medium) were added to the cells. After the incubation period of 24h and 48h, these conditions were removed, and the cells were trypsinized with trypsin 0.05%, and then counted, with the addiction of trypan blue,

to distinguish the cells with a compromised membrane from the others. The percentage of viable cells was then calculated.

2.18 Curcumin neuroprotection assays

For these assays, various concentrations of curcumin-loaded exosome-like liposomes with and without DODAP were used. In order to understand which concentrations of curcumin would present no cytotoxic effects to the cells, three concentrations of free curcumin at the concentrations of 8 μM and 20 μM were tested. Exosome-like liposomes with the least toxic concentrations of curcumin were then incubated with the cells, and the cytotoxicity was measured after 24 h.

For all the assays, cells were plated at the density of 1×10^5 cells/well in 24 well plates. After overnight stabilization, the cells were incubated with the exosome-like liposomes and the respective controls. For the induction of oxidative stress, 1 mM of t-BHP was added to SH-SY5Y cells after contact with the exosome-like liposomes. For the resazurin and AO/PI assays, the medium with the compounds was removed from the cells, and fresh medium containing t-BHP was added to induce oxidative stress. Fresh medium without t-BHP was added to the controls. After 2 h of incubation, the medium was removed for all conditions and 500 μl of resazurin at $2.4 \times 10^{-4}\text{M}$ dissolved in medium was added into each well. The cells were in contact with resazurin for 2 h. 100 μl of each sample, in triplicates, were transferred to a 96 well fluorescence plate. The fluorescence was the measured at $\lambda_{\text{exc}}=420$ nm and $\lambda_{\text{em}}=520$ nm.

For the AO/PI assay, after the incubation with t-BHP, 25 μl of PI at 50 μM were added for each well, and the plate was left in the dark at 37° C for 15 min. Then, aliquots of 25 μl of acridine orange at 50 μM were added to the plate and incubated for another 15 min. The fluorescence was then visualized using FITC and TRITC filters in a fluorescence microscope.

For the DCF assay, the medium was removed and 200 μl of DCF at the concentration of 100 μM were added to each well. The cells were left in the dark for 30 min at 37° C. Then, DCF was removed and 300 μl of a solution of t-BHP 1 mM in medium was added to each well and left to react for 15 min. The cells were then lysed with 350 μl of DMSO:PBS 1:1 (v:v) under agitation for 10 min. The fluorescence was then measured at $\lambda_{\text{exc}}=485$ nm and $\lambda_{\text{em}}=538$ nm.

3 Results

The physico-chemical properties of the exosome-like liposomes and curcumin-loaded exosome-like liposomes with and without DODAP, such as their size, polydispersity and surface charge were addressed. After verifying the encapsulation efficiency of curcumin in the exosome-like liposomes, they were incubated in SH-SY5Y cell to verify their neuroprotective effects against the induction of oxidative stress.

3.1 Empty and curcumin loaded exosome-like liposomes

Empty exosome-like liposomes were prepared by the ethanol injection method and were then purified, in a size exclusion column. The ethanol injection technique is an highly utilized technique that is easy to scale up and produces small liposomes, with low polydispersity^[129]. When the lipids reach the aqueous solution, they immediately organize into structures such as liposomes. Although this is a highly tunable technique, since various parameter such as temperature, lipid concentration and percentages, stirring velocity, or even the properties of the buffer, this also means that this technique can be less reproducible method than, for example, the extrusion method^[130]. Although this technique has some disadvantages, the overall simplicity, the fast implementation and the fact that it does not cause lipid degradation or oxidative alteration, makes it an interesting and widely used technique^[131].

3.1.1 Size, PDI and zeta potential of empty and curcumin-loaded exosome-like liposomes

Size, PDI and zeta potential measurements (**figure 9**) were then carried to assess physicochemical properties of the purified exosome-like liposomes. The same procedure was applied to curcumin-loaded exosome-like liposomes.

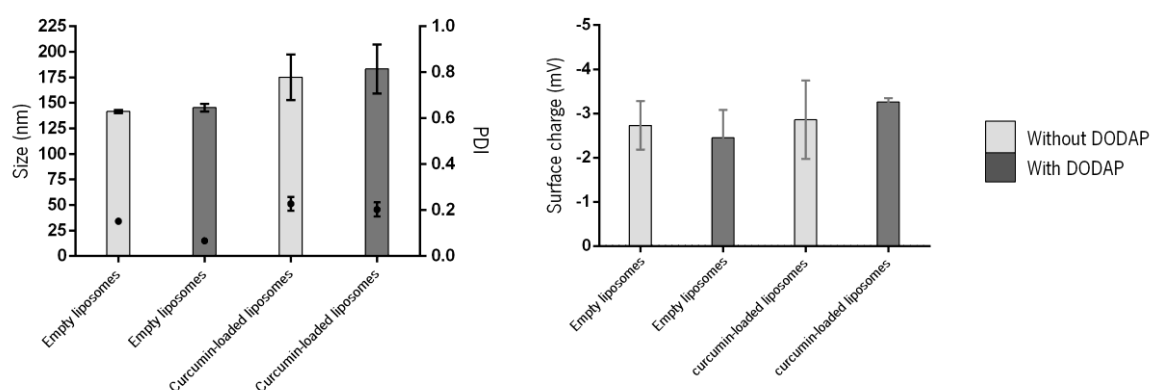


Figure 9: Size (bars), polydispersity (PDI; dots) and surface charge of empty and curcumin-loaded exosome-like liposomes, with and without DODAP.

Figure 9 illustrates significant differences in size between exosome-like liposomes and curcumin-loaded exosome-like liposomes, for both exosome-like liposome formulations. The encapsulation of curcumin seems to be causing a rearrangement in the exosome-like liposomes' structure, leading to bigger sizes and higher polydispersity index. There are no significant differences between exosome-like liposomes (with and without DODAP) in their charge, polydispersity and surface charge.

3.1.2 Storage stability of empty and curcumin-loaded exosome-like liposomes

The stability of the exosome-like liposomes was measured over time as depicted in **figures 10 and 11**. Exosome-like liposome stability is an important property for their storage, as stable exosome-like liposomes should retain their encapsulated contents. The more shelf life these nanoparticles have, the more time they can be stored while still retaining their properties and thus potentially applicable for therapeutic purposes.

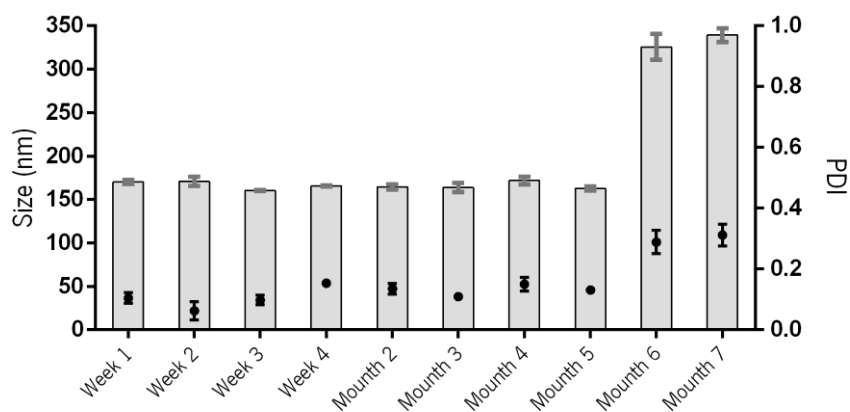


Figure 10: Size stability of empty liposomes without DODAP.

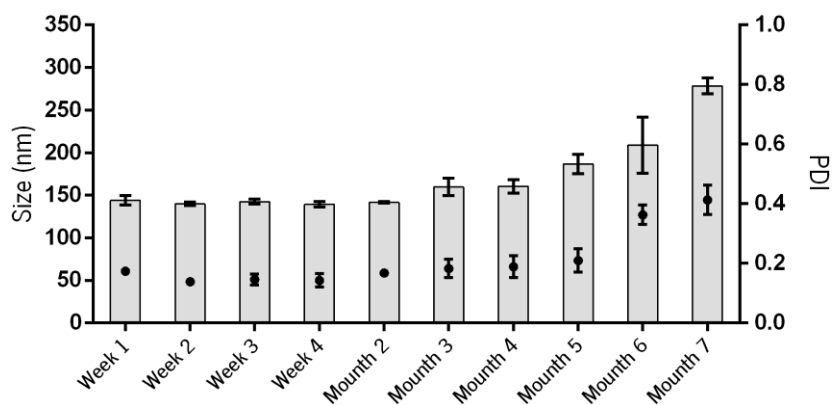


Figure 11: Size stability of empty liposomes with DODAP.

By analyzing **figures 10 and 11**, it is possible to verify that 6 months after their production, the exosome-like liposomes begin to lose stability, as indicated by a high polydispersity value. The size of the exosome-like liposomes seems to increase over time, which may be due to some level of aggregation in solution as the exosome-like liposomes become destabilized.

3.1.3 Curcumin encapsulation efficiency

Samples were analyzed before and after purification in the molecular exclusion column. The encapsulation percentages were calculated by comparing the unpurified samples with the purified ones. The results obtained are shown in **Table 8**.

Table 3: Curcumin encapsulation efficiency of samples with and without DODAP in the formulation ($\lambda_{exc}=420\text{nm}$; $\lambda_{em}=520\text{nm}$).

Samples	Encapsulation efficiency (%)
Exosome-like liposomes without DODAP	88.10
Exosome-like liposomes with DODAP	93.60

It is possible to verify a high encapsulation efficiency for both formulations, which is slightly higher for the formulation with DODAP. The high hydrophobicity of curcumin may be the most important factor for encapsulation.

3.1.4 F-TIR assay

The freshly produced curcumin-loaded exosome-like liposomes were tested along with empty exosome-like liposomes and free curcumin. **Figure 12** shows the absorbance spectra of the three samples. In the wavelength between 1900 and 3000 shows the peaks of exosome-like liposomes. The rest of the peaks show the links between curcumin and the exosome-like liposomes. The highest absorbance peak was at 1419. The spectra of curcumin-loaded exosome-like liposomes clearly show the successful incorporation of curcumin in the formulation.

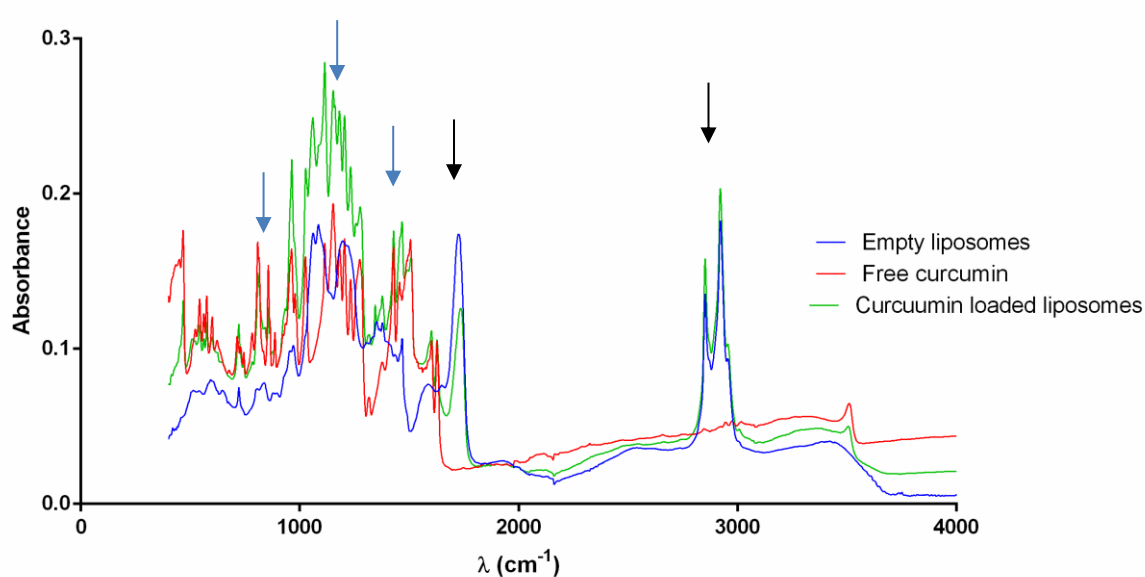


Figure 12: F-TIR absorbance spectra of free curcumin, empty exosome-like liposomes and curcumin-loaded exosome-like liposomes. The black arrows show the peaks where the presence of the exosome-like liposomes is visible, and the blue arrows indicate the presence of curcumin.

3.1.5 Resazurin assay

Resazurin assay was used to test cell viability, related to cellular metabolism. Two controls were used: one with HEPES at the percentage of the most concentrate liposome sample:18% (v/v), and the death control with 30% (v/v) DMSO.

After the incubation period, fluorescence at 590nm was measured and the percentage of cell survival was expressed normalized against the negative control (100% viability). The results were expressed as percentage of cell survival for each timepoint (24h; 48h and 72h).

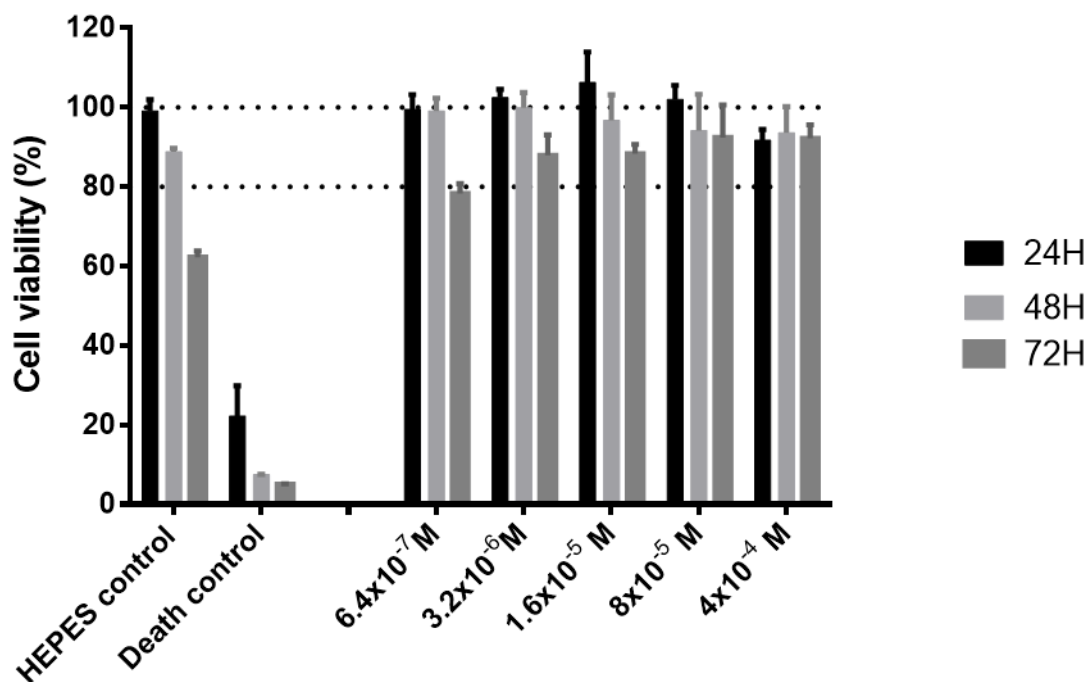


Figure 13: Viability assays of exosome-like liposomes with DODAP in L929 cell line. All concentrations of exosome-like liposomes with DODAP induce little to no cytotoxicity. These exosome-like liposomes show little toxicity that does not seem to be correlated with their concentration, at the tested values.

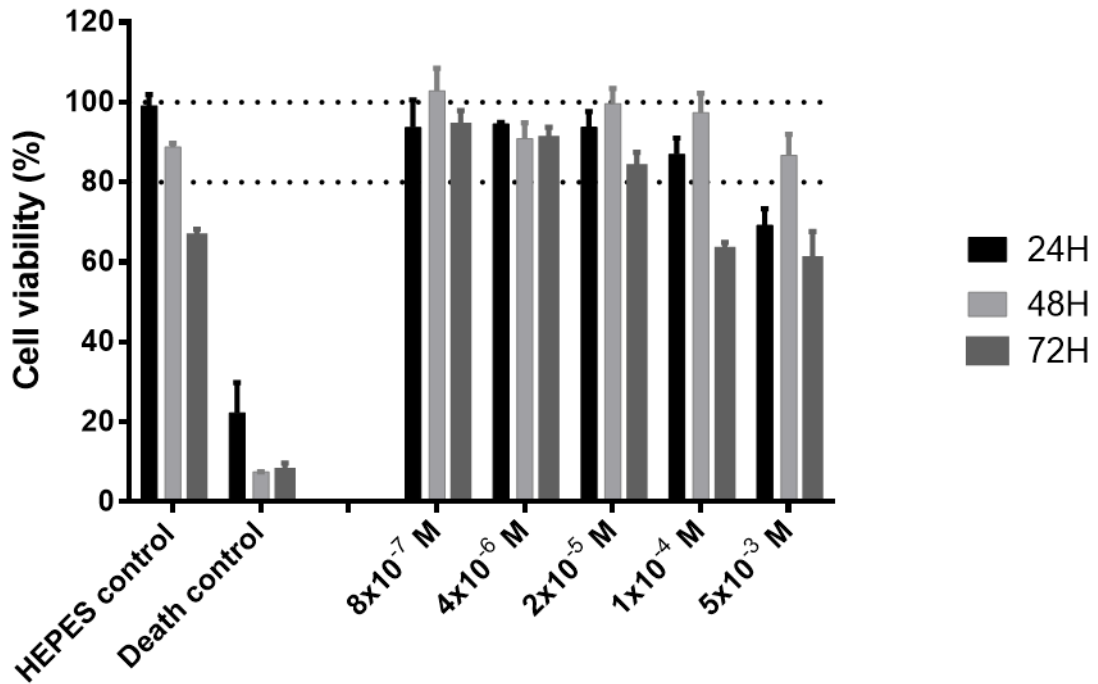


Figure 14: Viability assays of exosome-like liposomes without DODAP in L929 cell line; All concentrations of exosome-like liposomes without DODAP induce little to no cytotoxicity. The two most concentrated samples of these exosome-like liposomes seem to induce more toxicity than all the other samples.

The results clearly show that exosome-like liposomes with and without DODAP have little toxicity towards this cell line. Exosome-like liposomes with DODAP induce low cytotoxicity for all the concentrations tested, with most of them leading to cell viability above 80% in all the assays.

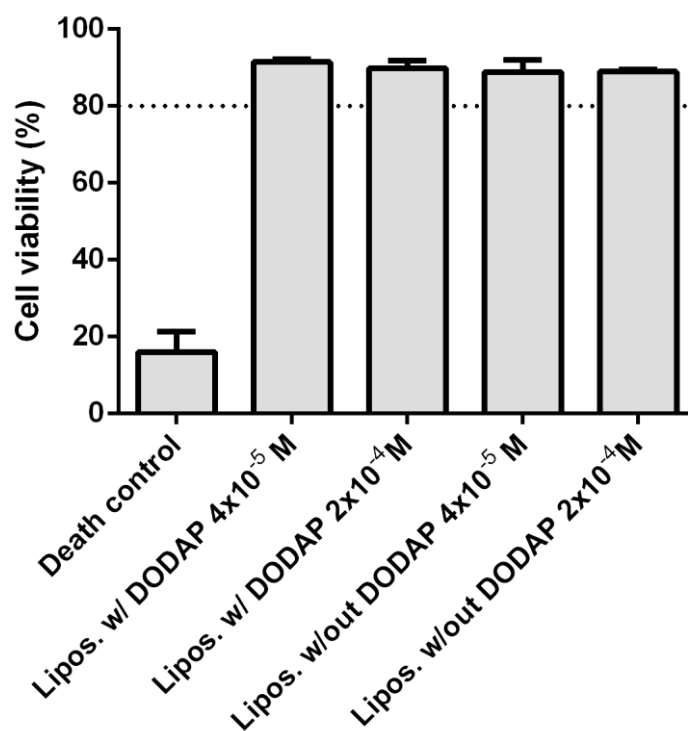


Figure 15: Cytotoxicity of curcumin-loaded exosome-like liposomes in SH-SY5Y cell line.

The same assay was performed in SH-SY5Y cells, with only the two highest concentrations of exosome-like liposomes with and without DODAP being tested, as shown in **figure 15**, for validation of the results obtained thus far. In this cell line, the exosome-like liposomes also do not induce significant toxicity for the cells. For the exosome-like liposomes without DODAP it is evident that their toxicity in this cell line is significantly less than towards the L929 cell line.

3.1.6 Trypan blue assay

This assay was performed to study the plasma membrane's integrity, when the cells were exposed to the exosome-like liposomes.

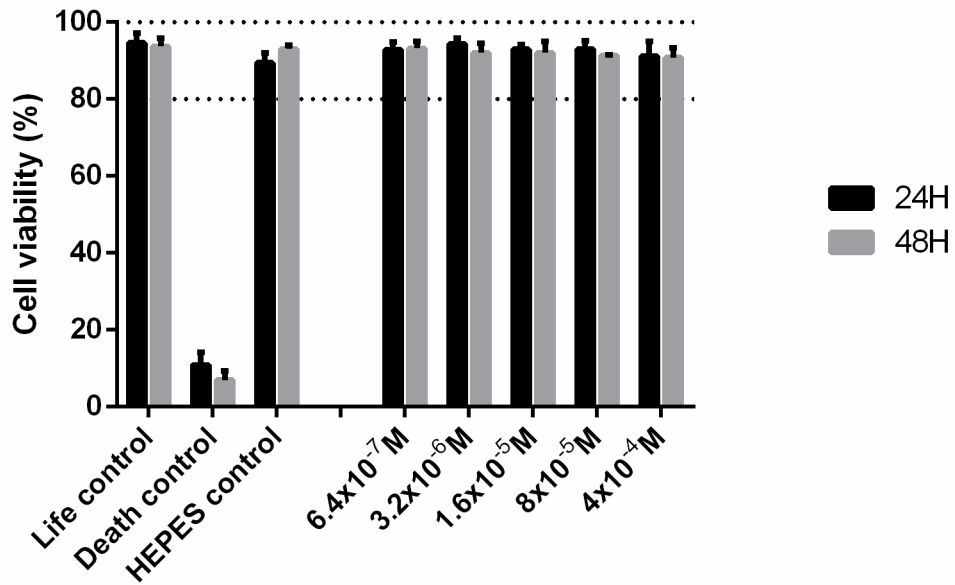


Figure 16: Percentage of unmarked cells when incubated with exosome-like liposomes with DODAP. The cells were counted, and the percentage was expressed considering the percentage of unmarked in relation to the total number of cells.

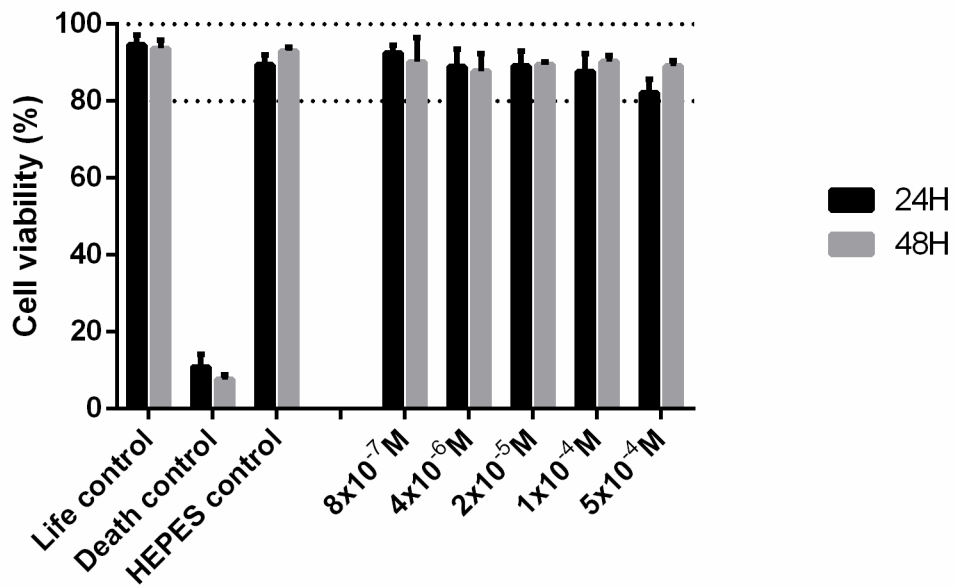


Figure 17: Percentage of unmarked cells when incubated with exosome-like liposomes without DODAP. The cells were counted, and the percentage was expressed considering the percentage of unmarked in relation to the total number of cells.

Since this dye is unable to penetrate the well-preserved plasma membrane, viable cells will not incorporate this dye. However, cells with a compromised plasma membrane will be stained blue since the dye can easily cross their damaged membrane.

The results obtained further prove that both exosome-like liposomes show little to no cytotoxicity. None of the exosome-like liposome concentrations, both with and without DODAP induce more than 20% of cell death. In this assay, exosome-like liposomes without DODAP do not induce cell permeability in the two most concentrated samples, in contrast to the little metabolic damage they cause, as measured by the resazurin assay. Even though this difference is small, this can indicate that these exosome-like liposomes more directly affect metabolism than cause membrane damage. When comparing to viability assays, for the two higher concentrations of exosome-like liposomes without DODAP, it is evident that in this assay, cells incubated with exosome-like liposomes at those concentrations are more viable.

3.1.7 Curcumin internalization assay

In order to determine if the exosome-like liposomes can successfully deliver curcumin to cells, SH-SY5Y were incubated with loaded exosome-like liposomes. Free curcumin was used as a control for the internalization of curcumin with the exosome-like liposomes. **Figure 18** shows the internalization of this molecule for the various concentrations at 2h and 4 h of incubation.

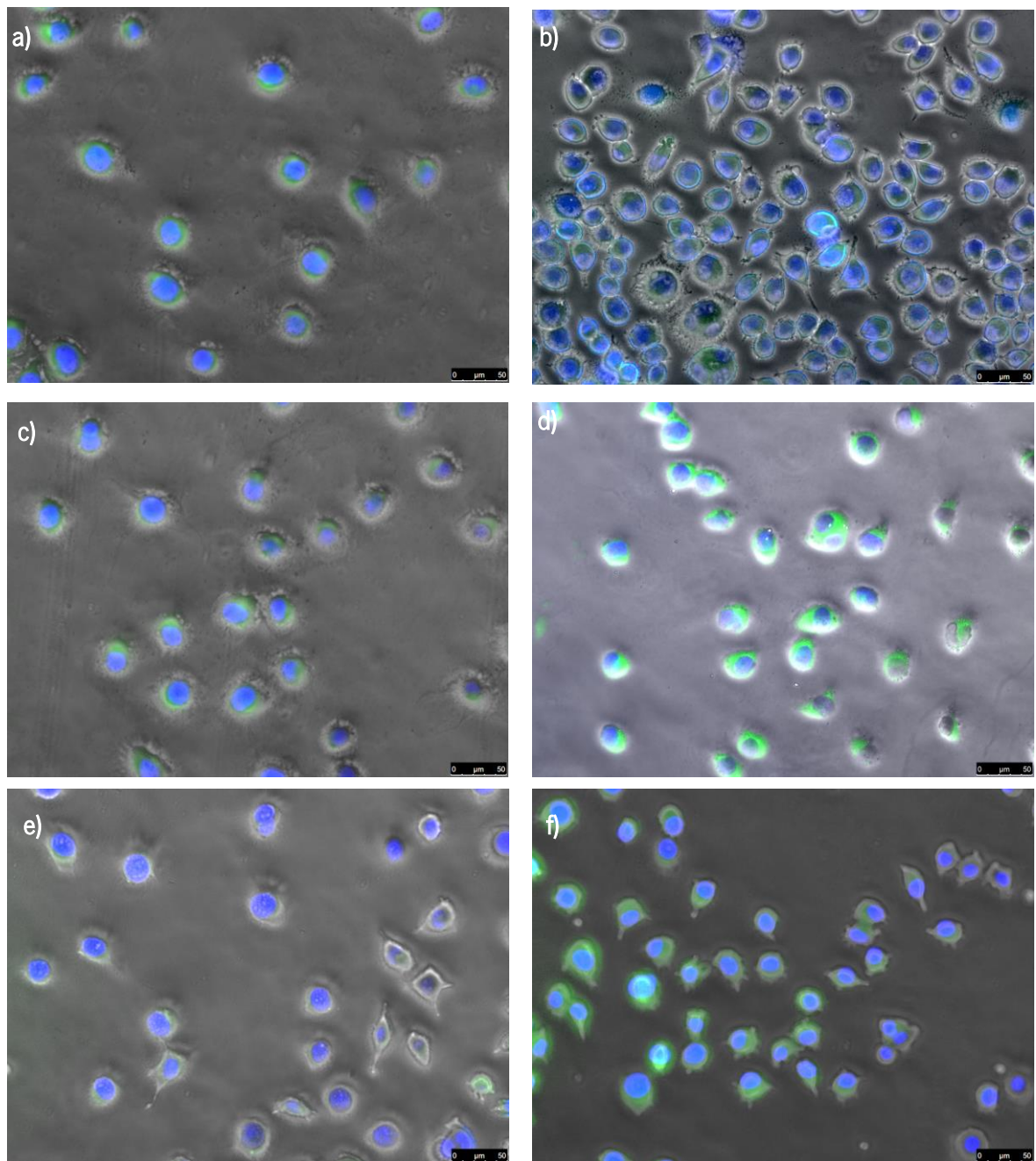


Figure 18: Curcumin internalization in SH-SY5Y cells: a), c) and e) 2h of incubation and b); d) and f) 4h of incubation. a) and b) represent free curcumin 20 μM ; c) and d) liposomes without DODAP with 20 μM of curcumin and e) and f) liposomes with DODAP with 20 μM of curcumin.

We verified that there are apparent differences between these two timepoints in terms of curcumin internalization. After 4 h, curcumin seems to be more internalized by the cells. As visible in the figure, there seems to be a higher incorporation of curcumin into the cells for the curcumin-loaded exosome-like liposomes than for free curcumin.

3.1.8 Curcumin neuroprotection assay

In order to verify which was the maximum concentration of curcumin that could be used safely in this cell line, a cytotoxic test with 3 concentrations of free curcumin was performed. The obtained results can be found in **figure 19** where we can see that the only concentration that does not induce cytotoxicity was 8 μM .

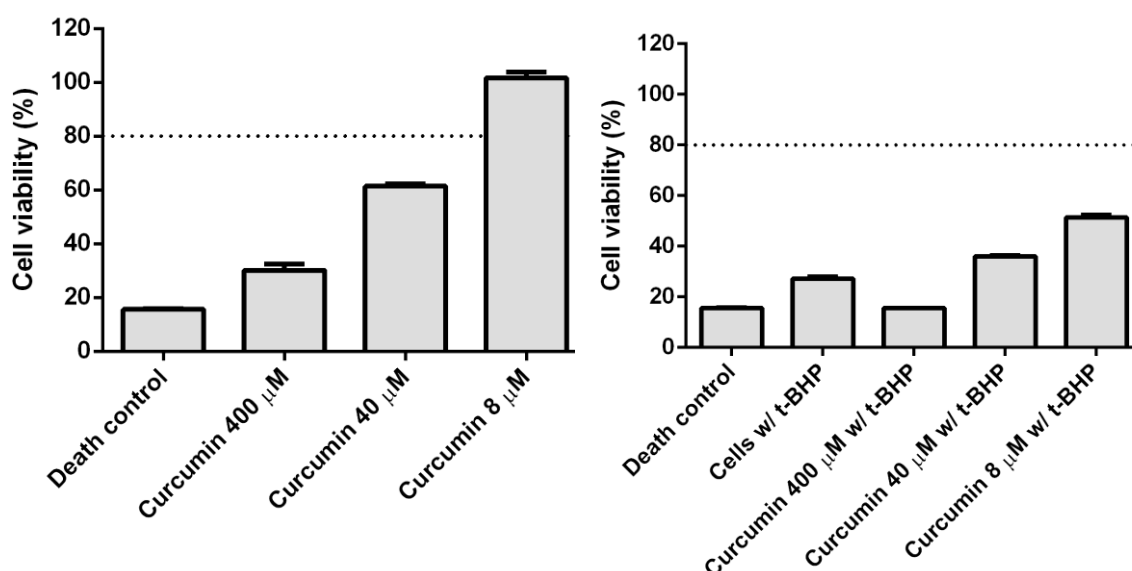


Figure 19: Effects in cell metabolism when SHSY-5Y cells are incubated with three different concentrations of curcumin (400 μM , 40 μM and 8 μM). The oxidative stress inducer was t-BHP at 1 μM .

A neuroprotective assay was also performed for similar concentrations of free curcumin. It is evident that the only concentration with significant differences from the control with t-BHP is 8 μM . At this concentration, curcumin is non-cytotoxic, contrary to the others, protecting cells from the oxidative insult.

After verifying which range of concentrations were safe to cells, a cytotoxicity assay, in the same conditions, with the same controls, was performed to evaluate cellular response to exosome-like liposomes containing similar concentrations of curcumin. These results are presented in **figure 20**.

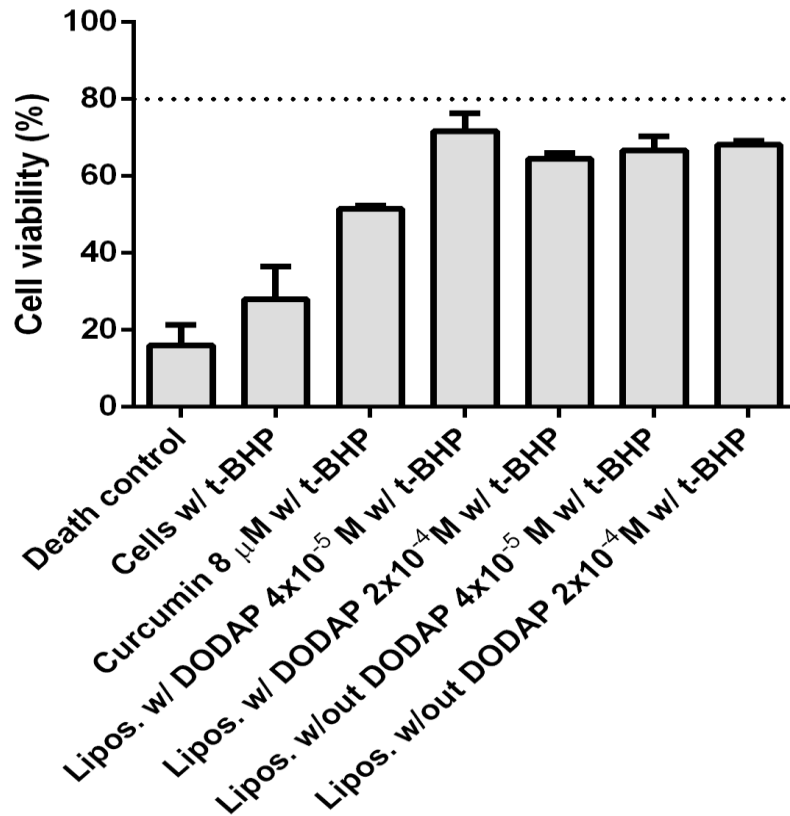


Figure 20: Neuroprotective effects of exosome-like liposomes with encapsulated curcumin in SH-SY5Y cells. The oxidative stress inducer used was 1 μ M t-BHP.

With the analysis of these results we can conclude that both formulations are effective in protecting the cells against the oxidative insult applied. These results show that curcumin-loaded exosome-like liposomes provide better neuroprotection against oxidative stress than the free curcumin. Based on the fact that both concentrations of curcumin in the exosome-like liposomes have similar effect, we can postulate that this outcome is not dependent of the curcumin concentration, at least above the concentration of 4×10^{-5} M. The two formulations also produce similar results.

3.1.9 Reactive Oxygen Species (ROS) generation in SH-SY5Y cell line

The probe DCFH-DA was used to evaluate the accumulation of reactive oxygen species in SH-SY5Y cells. The results shown in **figure 21** indicate that pre-incubation with exosome-like liposomes with curcumin reduces the production and accumulation of ROS in SH-SY5Y cells exposed to t-BHP.

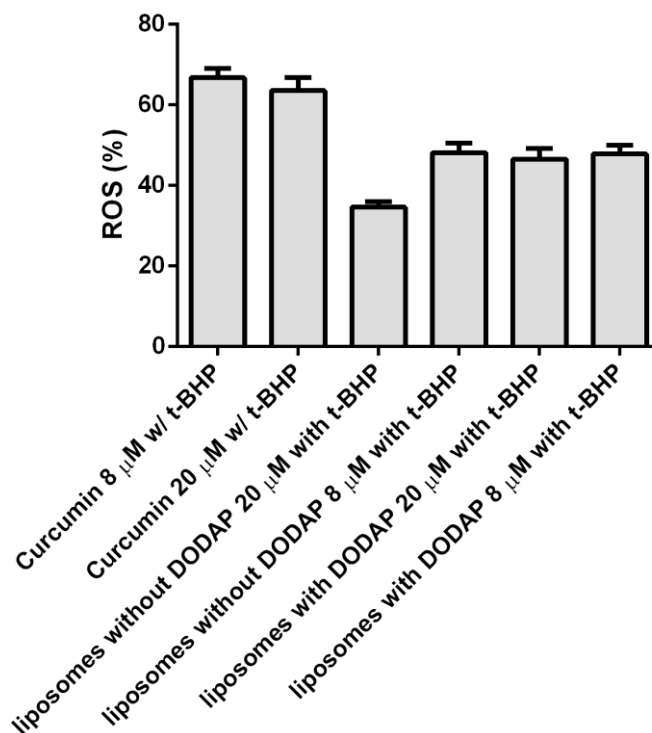


Figure 21: Percentage of ROS produced in SH-SY5Y cells in each condition. The percentage is expressed relative to the control with t-BHP.

By analyzing **figure 21**, it becomes clear that there is a clear reduction in ROS production in the SH-SY5Y cell line when incubated with the curcumin-loaded exosome-like liposomes. There is a significant difference in the results obtained with the exosome-like liposomes loaded with 20 μM of curcumin in comparison with the other exosome-like liposomes tested. In short, these exosome-like liposomes seem to confer better protection in neural cells than the other exosome-like liposomes tested or free curcumin, in neural cells exposed to oxidative insult.

3.1.10 Acridine orange/ Propidium iodide assay

To understand if the protection conferred by the loaded exosome-like liposomes could translate into a reduction of apoptosis due to the oxidative stress, the neural cells were stained with both acridine orange and propidium iodide. The use of these two molecules to evaluate apoptosis was described in the literature^[132], providing a successful distinction between apoptotic and non-apoptotic cells. Acridine orange is membrane-permeable, so it can be incorporated by live cells and stain the cell nuclei green. The identification of non-viable cells was addressed with propidium iodide, as this dye is not membrane-permeable and can only stain the nuclei blue, when the cells are compromised

and their membrane is not intact^[132]. As shown in **figure 23** untreated cells are majorly stained green, with few apoptotic cells, while the control with t-BHP a great portion of the cells are stained red, a clear marker of apoptosis. Nevertheless, some cells treated with exosome-like liposomes with either of the two tested concentrations of curcumin, for both formulations, become apoptotic. The percentage of apoptotic cells for these conditions is however substantially lower than for the negative control.

In **figure 22**, it is evident that the control with t-BHP presents more apoptotic cells than the control where cells are incubated only with medium. The incubation of free curcumin prior to induction of oxidative stress leads to a lower number of apoptotic cells. The incubation of cells with the exosome-like liposomes lead to a higher neuroprotection, translated into cell viability levels similar to that of the positive (life) control.

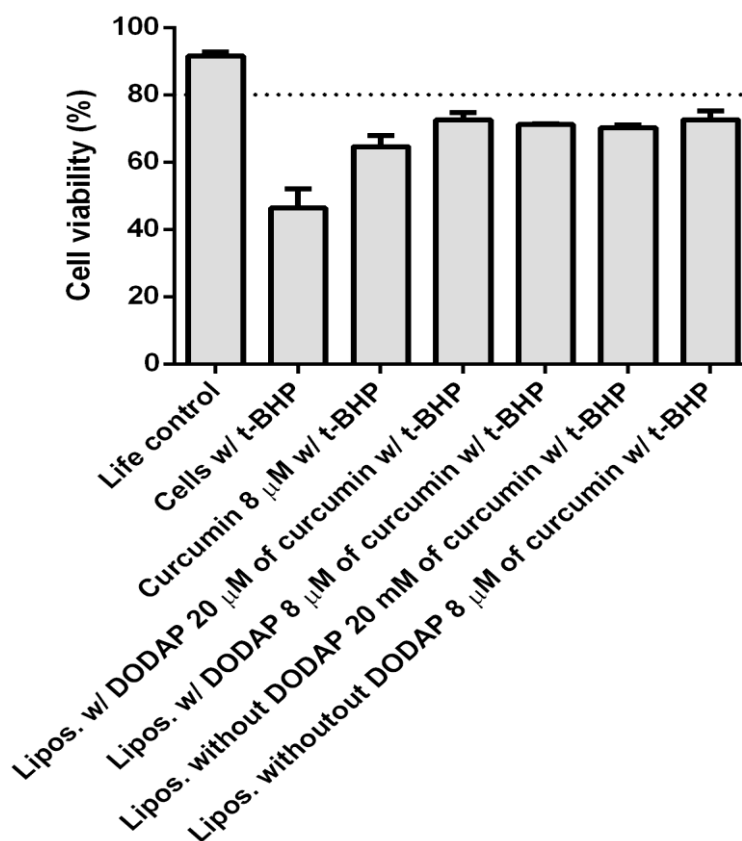


Figure 22: Percentage of non-apoptotic cells for each condition in SH-SY5Y cells.

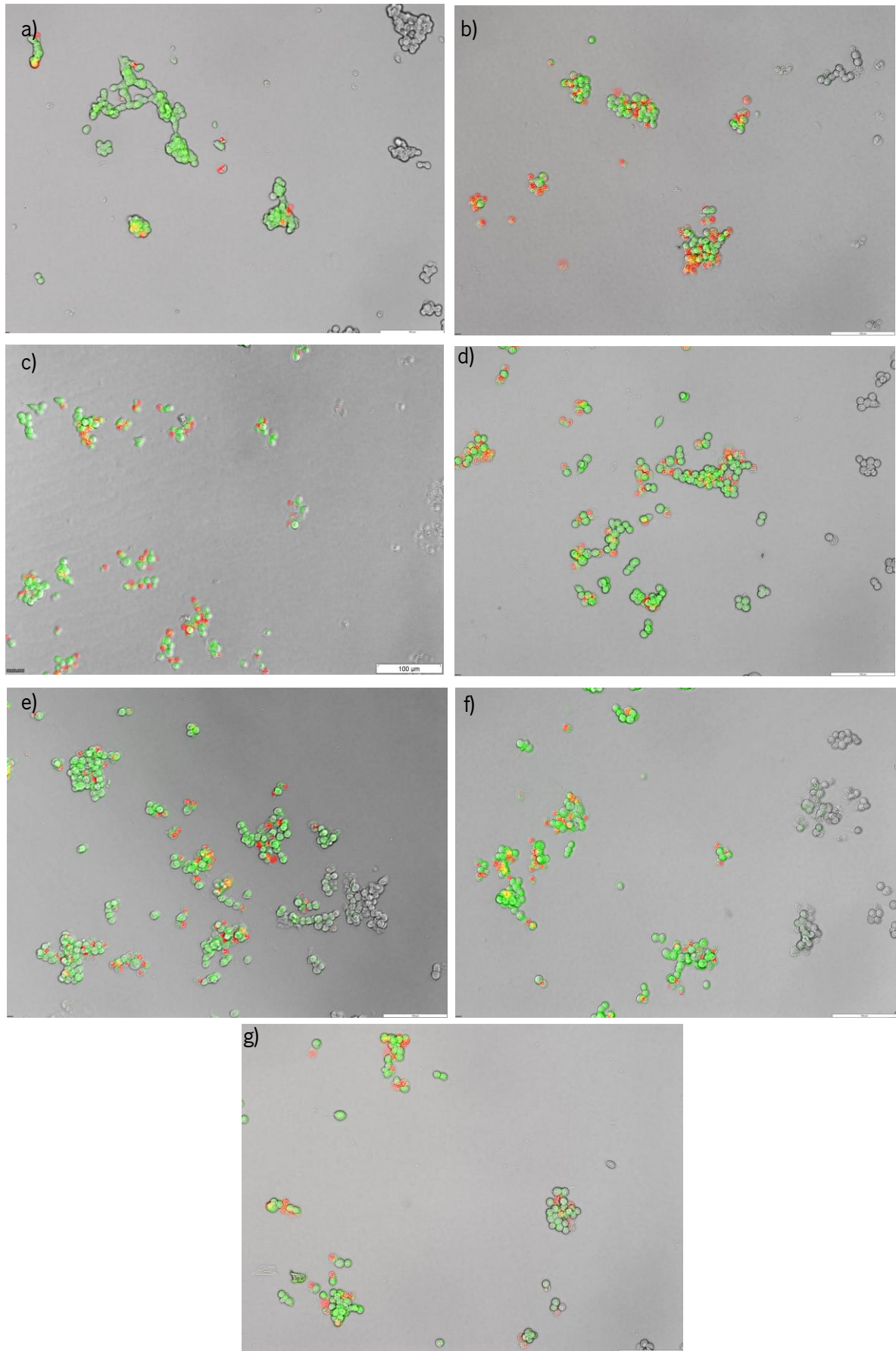


Figure 23: Apoptotic SH-SY5Y cells incubated with a) only medium; b) medium with t-BHP 1 mM; c) h) free curcumin 20 µM; d) 20 µM of curcumin loaded liposomes without DODAP; e) 8 µM of the previous liposomes; f) 20 µM of curcumin loaded liposomes with DODAP; g) 8 µM of the previous liposomes.

By analyzing **figure 22 and 23**, it is evident that cells incubated with curcumin-loaded exosome-like liposomes are less prone to enter late apoptosis than cells exposed only to the oxidative insult. It is also clear that the curcumin-loaded systems are more efficient than free curcumin. No differences in neuroprotection capacity were found between the 2 concentrations of curcumin loaded into exosome-like liposomes, or between exosome-like liposomes with and without DODAP.

3.2 siRNA exosome-like liposomes

3.2.1 Size, PDI and zeta potential of siRNA exosome-like liposomes

The size and zeta potential of the siRNA-loaded exosome-like liposomes without DODAP at diverse concentrations ($1 \times 10^{-5} \text{M}$; $5 \times 10^{-5} \text{M}$; $1 \times 10^{-4} \text{M}$ e $2 \times 10^{-4} \text{M}$) was measured in order to address differences in size, polydispersity and superficial charge. These differences are shown in the graphics of **figure 24**. Every sample was evaluated in the same concentration and conditions, only varying the concentration of siRNA encapsulated.

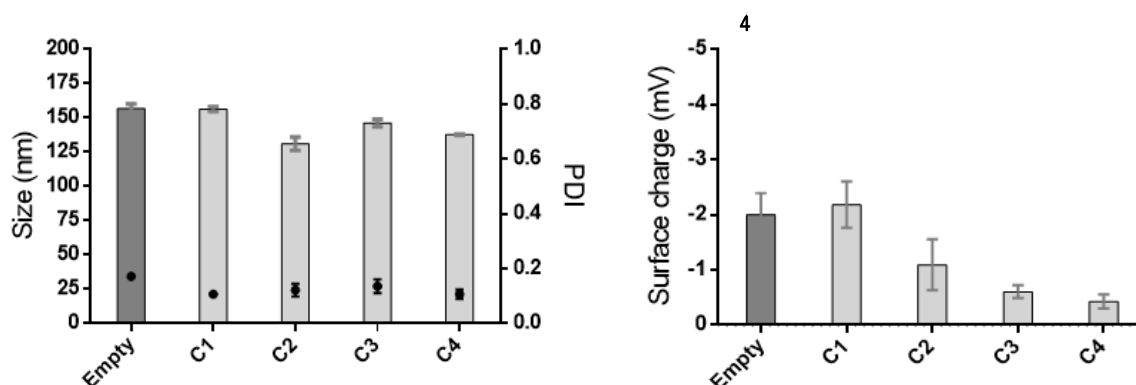


Figure 24: Size (bars), polydispersity and zeta potential (dots) of exosome-like liposomes without DODAP and with rising concentrations of siRNA (C1= $4.10 \times 10^{-6} \text{M}$; C2= $5 \times 10^{-6} \text{M}$; C3= $1 \times 10^{-5} \text{M}$ e C4= $2 \times 10^{-5} \text{M}$).

There is a tendency of positive correlation between increasing surface charge and increasing concentrations of siRNA. However, slight differences in surface charge of the various exosome-like liposomes are noticeable, being less negative with increasing siRNA concentrations

3.2.2 siRNA encapsulation efficiency

For the verification of the siRNA encapsulation efficiency with the RiboGreen® assay, the only free, non-encapsulated siRNA can bind to the dye and provide a measurable fluorescence signal. For this effect, after the encapsulation of siRNA and the separation of the free and encapsulated fractions, the exosome-like liposomes were destabilized with different types of detergents, for subsequent detection.

Then, the size and PDI of the samples after the treatment with the detergents were measured, in order to detect which detergent would cause greater destabilization. The results are found in **figure 25**, as a graphical representation of the size populations of each sample.

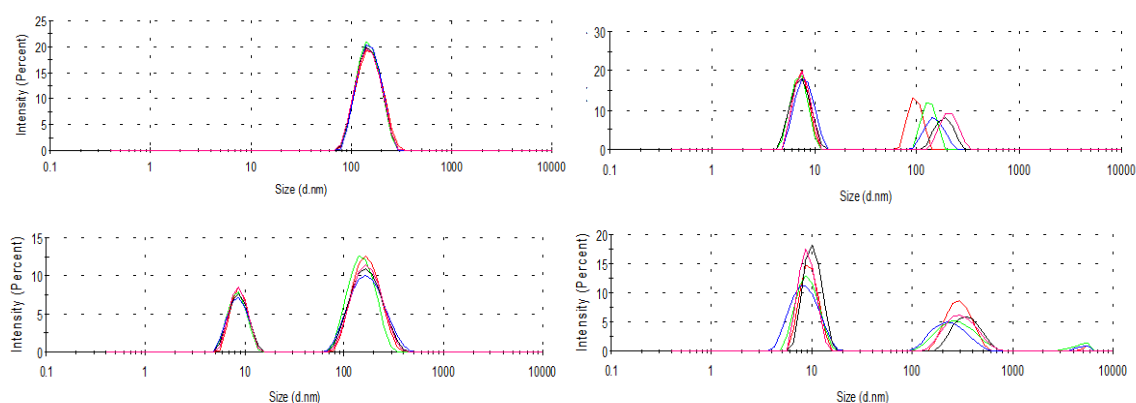


Figure 25: Liposomes with the initial formulation in HEPES buffer with a siRNA concentration of 4.10×10^{-5} M after heating, vortexing, and cooling 5 min on ice: a) liposomes without detergent; b) liposomes with C12E8; c) with Tween 20 and d) with Triton 10x.

In **figure 25** we can clearly detect two or more separate populations, after exosome-like liposomes were treated with the detergents. The population with the smaller size should represent the detergents' micelles, since they are known to have a much smaller size than the liposomes^[133]. It is clear that the exosome-like liposomes treated with C₁₂E₈ are the most destabilized as they present more populations, with a wide range of sizes.

The efficiency of siRNA encapsulation was calculated using the procedure previously described. After the destabilization of the exosome-like liposomes, siRNA fluorescence was measured using the RiboGreen® dye. The same measurements were performed for the control containing only

water and RiboGreen®, and another control containing water, RiboGreen® and the chosen detergent C₁₂E₈. The percentages of siRNA encapsulated in each exosome-like liposome are shown in **table 4**. siRNA encapsulation efficiency was determined after the purification on the molecular exclusion column, because with the method of passing the samples through amicon®, all samples had similar encapsulation efficiencies, all very close of 100%. We deduced that the separation of encapsulated and free siRNA, using this method, was not efficient. This was proved by the molecular exclusion method, with which we obtained very different encapsulation efficiencies.

Table 4 shows that there is almost 100% of siRNA encapsulation of siRNA in exosome-like liposomes containing DODAP. For the sample with 4.10x10⁻⁴ M of siRNA, there is a lower encapsulation efficiency of this molecule: 78.30%. The encapsulation efficiency was calculated for the concentrations of 5x10⁻⁵ M, 1x10⁻⁴ M and 2x10⁻⁴ M of siRNA in the exosome-like liposomes with the formulation without DODAP (0.24%, 0.20% and 0.47%, respectively). These encapsulation efficiencies help to prove that the exosome-like liposomes without DODAP are not suitable for encapsulation of siRNA.

The same study was performed with the exosome-like liposomes containing DODAP in the formulation using 3 different concentrations of siRNA.

Table 4: Encapsulation efficiency of 3 different siRNA concentrations in the exosome-like liposomes with DODAP.

siRNA concentration (M)	Encapsulation efficiency (%)
2.50x10 ⁻⁵	97.70
5x10 ⁻⁵	98.90
4.10x10 ⁻⁴	78.30

To prove this siRNA encapsulation efficiency, exosome-like liposomes with and without DODAP in the formulation were subjected to electrophoresis, which is represented in **figures 26 and 27**.

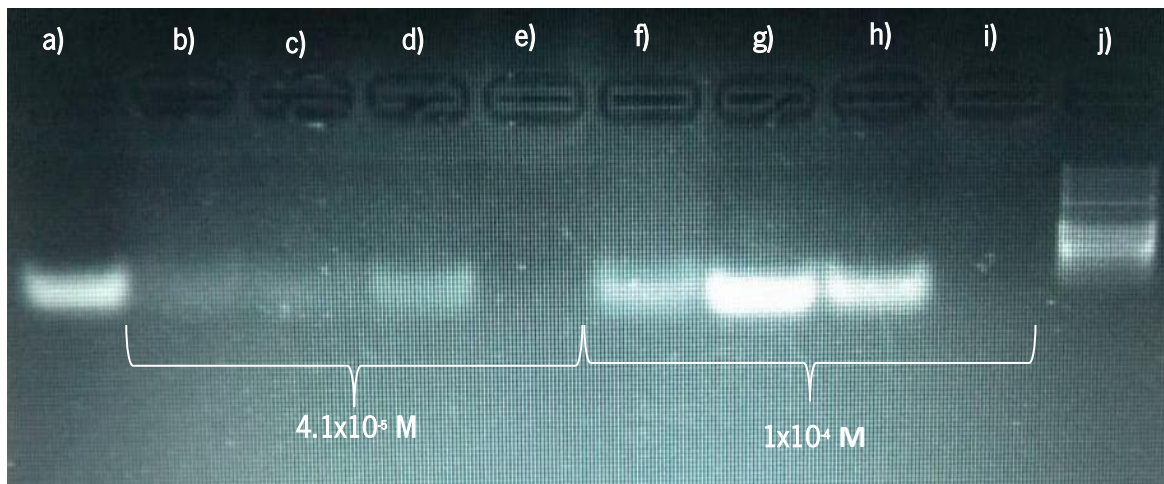


Figure 26: Electrophoresis of: a) siRNA 3.32 μg ; b) sample without purification; c) free part; d) encapsulated part; e) purified and treated with detergent; f) unpurified exosome-like liposomes; g) free part; h) encapsulated part; i) purified and treated with detergent exosome-like liposomes; j) ladder.

Samples of siRNA encapsulated in the exosome-like liposomes were evaluated with the initial formulation with two concentrations of siRNA: $5 \times 10^{-5} \text{ M}$ and $1 \times 10^{-4} \text{ M}$. Free siRNA was also included as control. All samples have the same theoretical amount of siRNA: $3.32 \mu\text{g}$. The encapsulated and free components correspond to exosome-like liposomes which were subjected to centrifugation in amicons® for purification. The encapsulated part corresponds to exosome-like liposomes retained in the filter and the free part is the remaining solution which passed through the pores of the filter.

After verification that the initial formulation did not encapsulate any siRNA, the efficiency of siRNA encapsulation was tested upon the addition of a cationic lipid to the formulation. This would cause the positive charge of the lipid to electrostatically attract the siRNA, which has negative charge. The chosen cationic lipid was DODAP, since its capacity to promote siRNA encapsulation is widely reported in the literature^[134]. The results of electrophoresis of siRNA lipoplexes made of DODAP-containing exosome-like liposomes are shown in **figure 27**.



Figure 27: Electrophoresis of a) siRNA 3.32 μ g; b) sample without purification; c) free part; d) encapsulated part; e) encapsulated part treated with $C_{12}E_8$; f) encapsulated part treated with Triton 10x; g) purified exosome-like liposomes; h) purified and treated $C_{12}E_8$ exosome-like liposomes; i) purified and Triton-treated exosome-like liposomes; j) ladder.

We observed an unquestionably effective encapsulation of siRNA with the addition of this lipid to the formulation, which can be verified in samples h) and i), where the appearance of a band indicates the presence of siRNA, in relation to a) to g) where, as expected, there is no free siRNA. After addition of any of the detergents, liposomal destabilization leads to a subsequent release of siRNA. Thus, it can be concluded that the addition of DODAP in the formulation was crucial for good siRNA encapsulation.

3.2.3 siRNA and curcumin co-encapsulation efficiency

DODAP exosome-like liposomes were used for the co-encapsulation of siRNA and curcumin, since they showed the highest efficiency of siRNA encapsulation. All samples were adjusted to the same lipid concentration. The results obtained are presented in **table 5**.

Table 5: Encapsulation efficiency of curcumin 1×10^{-3} M and 4.10×10^{-5} M siRNA in exosome-like liposomes with DODAP.

Samples	siRNA encapsulation efficiency (%)	Curcumin encapsulation efficiency (%)
Co-encapsulation of curcumin and siRNA	40.50	20.20
Separate encapsulation of curcumin and siRNA	78.30	93.60

An electrophoresis was performed using the same lipid concentration in each sample, so that variations in band intensity were only due to differences in siRNA encapsulation. Thus, it was possible to obtain a qualitative analysis of the siRNA content in the lipoplexes, and the differences between the separation techniques. Obtained results are shown in **figure 28**.

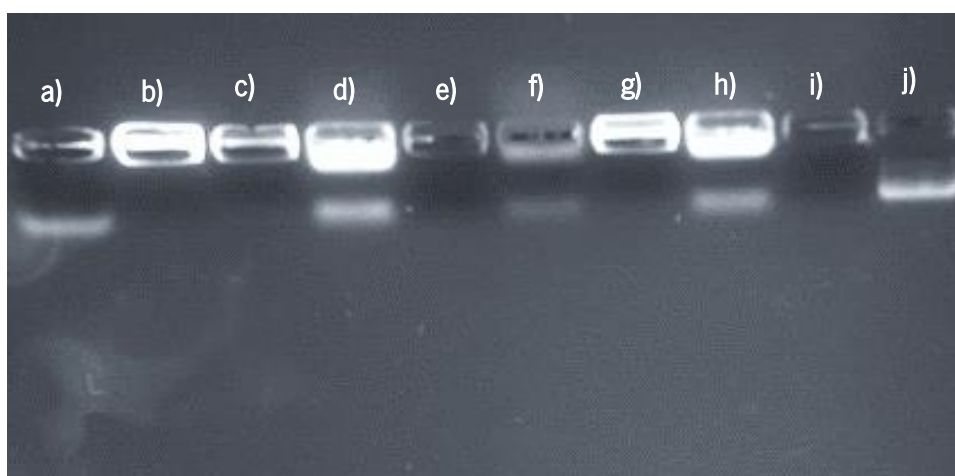


Figure 28: Electrophoresis of: a) siRNA; liposomes with DODAP b) without siRNA; c) non-purified; d) non-purified with C12E8; e) purified; f) purified with C₁₂E₈; g) encapsulated part; h) C₁₂E₈-treated encapsulated part; i) free siRNA from the liposomes passed through the amicon®; j) ladder.

These results are concordant with those obtained with the fluorescence analysis method using RiboGreen®. Thus, the percentage of co-encapsulation of siRNA and curcumin is 40.5% and 20.2% respectively. Since these values are considerably lower than those obtained with separate

encapsulation of the two molecules, the latter strategy was chosen and exosome-like liposomes containing each molecule were later mixed for a dual formulation.

4 Discussion

Exosome-like liposomes, with or without DODAP, encapsulating curcumin display similar size, PDI and surface charge, although of significantly higher size and PDI than exosome-like liposomes without any load. This effect of curcumin on liposome size and PDI was also seen by Yin *et al.*^[135] as their liposomes loaded with curcumin had a bigger size than unloaded ones. However, these exosome-like liposomes have a size below 200 nm, which is essential to be able to cross the blood brain barrier, and have a PDI close to 0.2, and so the sample is not very polydisperse^[136].

The encapsulation efficiency of curcumin for these systems is high, even for high concentrations. These encapsulation efficiencies are similar to those obtained by Riwang *et al.* that achieved 88,75% of curcumin in chitosan liposomes^[137]. Exosome-like liposomes containing DODAP have a slight superior encapsulation efficiency than the ones without this molecule in their constitution. As curcumin is less soluble in aqueous solutions^[138], preparation of exosome-like liposomes with the citrate buffer (pH 3.0) can make curcumin more likely to be internalized in the exosome-like liposomes. This can explain the higher encapsulation efficiencies for this molecule in exosome-like liposomes containing DODAP.

The F-TIR analysis shows, as marked by the arrows in **figure 12**, that some peaks are prominent in some wavelengths for each sample. As described in the literature^[139], curcumin has a peak in its F-TIR absorbance spectra in 1419 cm^{-1} . As is seen in **figure 12**, free curcumin and curcumin loaded exosome-like liposomes have some common peaks, proving that curcumin was indeed encapsulated in these exosome-like liposomes. The remaining peaks are all relative to the lipids that constitute the exosome-like liposomes. These peaks are marked with the black arrows and are coincident in the graphs of empty and loaded liposomes. Taken together, this proves that curcumin is encapsulated in the exosome-like liposomes.

As for the cytotoxic assays, we can assume that cell metabolism is not affected by liposome concentration up to 4 mM. Although also showing low cytotoxicity, samples containing higher concentrations of exosome-like liposomes without DODAP tend to induce more cytotoxicity. The two

higher concentration of these exosome-like liposomes (5 mM and 1 mM) lightly affect cell metabolism and viability, contrary to other exosome-like liposome concentrations. This was not observed with the trypan blue assay. The addition of DODAP to the formulation, potentially giving the exosome-like liposomes a positive surface charge, and potentially causing more cytotoxicity, due to interference with the membrane potential and with membrane function and integrity^[140]. However, this negative effect was not observed, and exosome-like liposomes with DODAP induce even less cytotoxicity than exosome-like liposomes without this positive lipid in the formulation. This fact can be justified with the use of low concentrations of DODAP and its low cytotoxicity by itself. In fact, liposomes with this lipid have been associated to a lower cytotoxicity compared to liposomes with other cationic lipids ^[141]. Furthermore, this molecule is only positively charged for acidic pH (3.0 or lower)^[142]. While these exosome-like liposomes were prepared in citrate buffer with pH 3.0, they were later purified in the molecular exclusion column, with HEPES buffer of pH 7.4. This could mitigate the positive charge of DODAP, making these exosome-like liposomes less problematic to exposed cells. The fact that these exosome-like liposomes are little to non-cytotoxic is further proven by the results in **figure 29**, supplementary data, where it can be seen that the cells maintain their normal morphology after 24 h, 48 h and 72 h of incubation with the exosome-like liposomes. Although the induction of some cytotoxicity, the HEPES should not be cytotoxic, as it is a biocompatible buffer, that can be used in some culture mediums and cell assays.

The curcumin-loaded exosome-like liposomes can deliver curcumin into the cells with more efficiency than what was reported by Li *et al.* in which only a similar transfection of free and liposomal curcumin in LoVo human colorectal cancer cells could be achieved^[143]. However, curcumin seems to not enter the nuclei, as seen in **figure 18**. These results are similar to those by Banderali *et al.* who reported perinuclear accumulation of curcumin ^[144]. The exosome-like liposomes and free curcumin accumulate inside the cells more strongly after 4 h of incubation. No apparent difference between the two types of exosome-like liposomes in delivery efficiency was noted.

Curcumin-loaded exosome-like liposomes also do not seem to induce cytotoxicity, provided that the concentration of curcumin in the exosome-like liposomes is lower than 20 μ M. There is evident toxicity of curcumin for values superior to 40 μ M (free curcumin) as evidenced by **figure 19**. Free curcumin is cytotoxic, as described by Woo *et al.* that demonstrated that, when treated with 50 μ M of curcumin, human renal carcinoma Caki cells would enter apoptosis, by activating caspase 3 cleavage of phospholipase C-g1 and DNA fragmentation^[145].

Curcumin-loaded exosome-like liposomes also do not seem to induce cytotoxicity, provided that the concentration of curcumin in the exosome-like liposomes is lower than 20 μM . There is evident toxicity of curcumin for values superior to 40 μM (free curcumin) as evidenced by **figure 19**. Free curcumin is cytotoxic, as described by Woo *et al.* that demonstrated that, when treated with 50 μM of curcumin, human renal carcinoma Caki cells would enter apoptosis, by activating caspase 3 cleavage of phospholipase C-g1 and DNA fragmentation^[145].

Curcumin-loaded exosome-like liposomes with and without DODAP contribute to a reduction of oxidative stress production and its consequent negative effect on cell metabolism in the SH-SY5Y neuronal cell line, which is proven by the resazurin, DCFH and Acridine orange assays. Daverey *et al.* also found that curcumin can alleviate oxidative stress and mitochondrial damage^[146]. Yin *et al.* also found that curcumin can protect SH-SY5Y cells against oxidative stress by up-regulating HO-1 expression^[147].

For lipoplex formation, DODAP was essential to give exosome-like liposomes a positive surface charge (**figure 23**), facilitating electrostatic encapsulation of siRNA. siRNA could be efficiently encapsulated in exosome-like liposomes with DODAP, with the least encapsulation efficiency for $4.1 \times 10^{-4} \text{ M}$ siRNA, possibly by reaching the saturation limit for encapsulation of this molecule.

To quantify the efficiency of siRNA encapsulation, the detergent with the best results was C_{12}E_8 . By analyzing the size of the exosome-like liposomes in **figure 25**, we can deduce that the detergents that cause greater destabilization in the exosome-like liposomes are C_{12}E_8 and Triton 10x. This was expected since these detergents are known to induce the fusion of liposomes into larger vesicles, posteriorly solubilizing them^[148]. It is possible to verify through PDI analysis of the samples treated with the various detergents that Triton should cause a greater destabilization of the exosome-like liposomes. However, it is notorious that this variation in polydispersity is greatly affected by the high number of detergent micelles, and not because of the substantial destabilization of the exosome-like liposomes. Although Tween 20 causes high polydispersity in the exosome-like liposomes, this is seen because there is a second population, corresponding to the detergent micelles, causing little to no liposomal destabilization. Moreover, studies show that this detergent has low destabilization efficiency^[149], so it was discarded. By analyzing the graph with detergent C_{12}E_8 , it is possible to substantiate that it caused greater destabilization, generating several populations of exosome-like liposomes, of different sizes.

This fact, together with a pronounced polydispersity, indicates that this detergent is the most suitable for the destabilization of this type of exosome-like liposomes.

The electrophoresis performed further corroborate the encapsulation of siRNA in exosome-like liposomes with DODAP and the impossibility to incorporate this molecule in exosome-like liposomes without DODAP. This could be due to a non-internalization of the siRNA in the exosome-like liposomes.

The co-encapsulation of siRNA and curcumin in exosome-like liposomes with DODAP was proven inefficient, with a drastic decrease in the incorporation of these molecules. The rearranging of the membrane by curcumin can be fundamental for the non-encapsulation of siRNA. Curcumin possibly mitigates the positive charge of the exosome-like liposomes, making siRNA encapsulation more difficult. As these molecules compete for incorporation into the membrane of exosome-like liposomes (siRNA at the surface and curcumin inside the membrane) the co-encapsulation of these molecules is not the best strategy. However, the parallel production of curcumin and siRNA-loaded exosome-like liposomes proved to be very efficient and the mixture of these exosome-like liposomes after their production is a promising and interesting approach for their later use in therapy.

Conclusions and future work

The physico-chemical properties of the exosome-like liposomes obtained by ethanol injection were studied using the DLS . The DLS measurements proved that the exosome-like liposomes could be used to cross the blood brain barrier, since their size is inferior to 200 nm. There were no significant differences in size and polydispersity between both formulations, and they both could efficiently encapsulate curcumin, with efficiencies superior to 80 %. The encapsulation of siRNA was only successful for exosome-like liposomes with DODAP, due to the positive charge of this lipid that could electrostatically bind this molecule to the exosome-like liposomes. The F-TIR measurements also proved that curcumin was encapsulated in exosome-like liposomes containing DODAP, and the electrophoresis proved that exosome-like liposomes without DODAP could not encapsulate it, while it was proved to be present in exosome-like liposomes with DODAP. These tests allowed us to conclude that exosome-like liposomes with DODAP were suitable to encapsulate both curcumin and siRNA, while exosome-like liposomes without DODAP could only encapsulate curcumin. The co-encapsulation

of siRNA and curcumin in exosome-like liposomes with DODAP was proved to be inefficient as the efficiency of encapsulation for both molecules was drastically inferior. For a possible therapy, it could be beneficial to encapsulate these molecules separately and administrate a mixture of exosome-like liposomes either with or without DODAP for curcumin and with DODAP for siRNA.

Neither of these exosome-like liposomes were proven to be cytotoxic to the L929 or SH-SY5Y cell lines. In fact, even though DODAP is known to be cytotoxic (even though it is less cytotoxic than other common positively charged lipids used in liposome preparation), in the literature, due to its high positive charge^[150], we found that exosome-like liposomes without DODAP were more toxic for the two highest concentrations. All these factors make exosome-like liposomes with DODAP better carriers for the encapsulation and delivery of curcumin and siRNA.

The curcumin exosome-like liposomes successfully penetrate the cell membrane and deliver curcumin in the cytoplasm, not the nuclei. For the neuroprotection assays, both exosome-like liposomes with curcumin loaded were tested. The results were similar for both formulations. These neuroprotective effects were proven by the diminishing of the ROS levels, the improved metabolic activity and the reduction of cells entering late apoptosis, after oxidative insult when cells were pre-incubated with exosome-like liposomes containing curcumin. This effect was also observed for free curcumin, although to a lesser extent than for the same quantity of curcumin delivered by the exosome-like liposomes. This can indicate that the exosome-like liposomes do not only protect curcumin from external threats, giving it stability and providing a carrier to transport it to the brain, but also allow the curcumin to be internalized into the cells and have better neuroprotection effects.

Further *in vivo* tests can be performed in order to test these exosome-like liposomes cytotoxicity and bioactivity. Zebrafish are an excellent model to test nanoparticles and can be an interesting vessel to verify the accumulation of these exosome-like liposomes.

4. Bibliography

- [1] Han, M.; Lee, E.; Koh, S. Current Opinion on the Role of Neurogenesis in the Therapeutic Strategies for Alzheimer Disease , Parkinson Disease , and Ischemic Stroke ; Considering

- Neuronal Voiding Function. *Int. Neurol. J.* **2016**, *20* (4), 276–287.
- [2] van Eijk, R. P. A.; Nikolakopoulos, S.; Ferguson, T. A.; Liu, D.; Eijkemans, M. J. C.; van den Berg, L. H. Increasing the Efficiency of Clinical Trials in Neurodegenerative Disorders Using Group Sequential Trial Designs. *J. Clin. Epidemiol.* **2018**, *98*, 80–88.
- [3] Walker, L. C.; Jucker, M. Neurodegenerative Diseases : Expanding the Prion Concept. *Annu. Rev. Neurosci.* **2015**, *38*, 87–103.
- [4] Brettschneider, J.; Tredici, K. Del; Virginia, M.-Y. L.; Trojanowski, J. Q. Spreading of Pathology in Neurodegenerative Diseases: A Focus on Human Studies. *Nat. Rev. Neurosci.* **2015**, *1*, 1–17.
- [5] Villar-Piqué, A.; Schmitz, M.; Candelise, N.; Ventura, S.; Llorens, F.; Zerr, I. Molecular and Clinical Aspects of Protein Aggregation Assays in Neurodegenerative Diseases. *Organization* **2010**, *3*(10), 3323–3331.
- [6] Qiu, C.; Kivipelto, M.; Von Strauss, E. Epidemiology of Alzheimer's Disease: Occurrence, Determinants, and Strategies toward Intervention. *Dialogues Clin. Neurosci.* **2009**, *11* (2), 111–128.
- [7] Adalier, N.; Parker, H. Vitamin E , Turmeric and Saffron in Treatment of Alzheimer ' S Disease. *Antioxidants* **2016**, *5* (40), 1–14.
- [8] Panahi, Y.; Mohammadhosseini, M.; Abadi, A. J. N.; Akbarzadeh, A.; Mellatyar, H. An Update on Biomedical Application of Nanotechnology for Alzheimer ' S Disease Diagnosis and Therapy. *Drug Res* **2016**, *66*, 580–586.
- [9] Santos, M. A.; Chand, K.; Chaves, S. Recent Progress in Multifunctional Metal Chelators as Potential Drugs for Alzheimer ' S Disease. *Coord. Chem. Rev.* **2016**, *327–328*, 287–303.
- [10] Minter, M.; Taylor, J.; Crack, P. The Contribution of Neuroinflammation to Amyloid Toxicity in Alzheimer's Disease. *J. Neurochem.* **2016**, *136*, 457–474.
- [11] Stocco, A.; Coppedè, F. Role of Epigenetics in Alzheimer ' S Disease Pathogenesis. *Neurodegener. Dis. Manag.* **2018**, *10* (5), 338–345.

- [12] Hsu, H. W.; Bondy, S. C.; Kitazawa, M. Environmental and Dietary Exposure to Copper and Its Cellular Mechanisms Linking to Alzheimer's Disease. *Toxicol. Sci.* **2018**, *163* (2), 338–345.
- [13] Kilian, J.; Kitazawa, M. The Emerging Risk of Exposure to Air Pollution on Cognitive Decline and Alzheimer's Disease – Evidence from Epidemiological and Animal Studies. *Biomed. J.* **2018**, *41* (3), 141–162.
- [14] Perrone, F.; Cacace, R.; Van Mossevelde, S.; Van den Bossche, T.; De Deyn, P. P.; Cras, P.; Engelborghs, S.; van der Zee, J.; Van Broeckhoven, C. Genetic Screening in Early-Onset Dementia Patients with Unclear Phenotype: Relevance for Clinical Diagnosis. *Neurobiol. Aging* **2018**, *69*, 292.e7-292.e14.
- [15] Ferrer, I. Defining Alzheimer as a Common Age-Related Neurodegenerative Process Not Inevitably Leading to Dementia. *Prog. Neurobiol.* **2012**, *97*(1), 38–51.
- [16] Vandenberghe, R.; Tournoy, J. Cognitive Aging and Alzheimer's Disease. *Postgrad. Med. J.* **2005**, *81* (956), 343–352.
- [17] Swerdlow, R. H. Is Aging Part of Alzheimer's Disease, or Is Alzheimer's Disease Part of Aging? *Neurobiol. Aging* **2007**, *28* (10), 1465–1480.
- [18] Bélanger, M.; Allaman, I.; Magistretti, P. J. Brain Energy Metabolism: Focus on Astrocyte-Neuron Metabolic Cooperation. *Cell Metab.* **2011**, *14* (6), 724–738.
- [19] Mergenthaler, P.; Lindauer, U.; A. Dienel, G.; Meisel, A. Sugar for the Brain: The Role of Glucose in Physiological and Pathological Brain Function. *Trends Neurosci.* **2013**, *36* (10), 587–597.
- [20] Carvalho, C.; Moreira, P. I.; Sena, C. M. Oxidative Stress : A Major Player in Cerebrovascular Alterations Associated to Neurodegenerative Events. *Front. Physiol.* **2018**, *9* (July), 1–14.
- [21] Angelova, P. R.; Abramov, A. Y. Role of Mitochondrial ROS in the Brain : From Physiology to Neurodegeneration. *FEBS Lett.* **2018**, *592*, 692–702.
- [22] Vargas, L. M.; Cerpa, W.; Muñoz, F. J.; Zanlungo, S.; Alvarez, A. R. BBA - Molecular Basis of Disease Amyloid- β Oligomers Synaptotoxicity : The Emerging Role of EphA4 / c-Abl Signaling in Alzheimer's Disease. *Mol. Basis Dis. J.* **2018**, *1864* (January), 1148–1159.

- [23] Ovsepiyan, S. V.; O'Leary, V. B.; Zaborszky, L.; Ntziachristos, V.; Dolly, J. O. Synaptic Vesicle Cycle and Amyloid β : Biting the Hand That Feeds. *Alzheimer's Dement.* **2018**, *14* (4), 502–513.
- [24] Mucke, L.; Selkoe, D. J. Neurotoxicity of Amyloid β -Protein: Synaptic and Network Dysfunction. *Cold Spring Harb. Perspect. Med.* **2012**, *2* (7), 1–17.
- [25] Kandimalla, K. K.; Scott, O. G.; Fulzele, S.; Davidson, M. W.; Poduslo, J. F. Mechanism of Neuronal versus Endothelial Cell Uptake of Alzheimer's Disease Amyloid β Protein. *PLoS One* **2009**, *4* (2), 1–20.
- [26] Selkoe, D. J. Physiological Production of the β -Amyloid Protein and the Mechanism of Alzheimer's Disease. *Trends Neurosci.* **1993**, *16* (10), 403–409.
- [27] Bayer, T. A.; Wirths, O. Intracellular Accumulation of Amyloid-Beta – a Predictor for Synaptic Dysfunction and Neuron Loss in Alzheimer's Disease. *Front. Aging Neurosci.* **2010**, *2*, 1–10.
- [28] McLean, C. A.; Cherney, R. A.; Fraser, F. W.; Fuller, S. J.; Smith, M. J.; Beyreuther, K.; Bush, A.; Masters, C. L. Soluble Pool of AB as a Determinant of Severity of Neurodegeneration in Alzheimer's Disease. *Ann Neurol (In Press)*. **1999**, *46* (6), 860–866.
- [29] Harrison, J. R.; Owen, M. J. Alzheimer's Disease: The Amyloid Hypothesis on Trial. *Br. J. Psychiatry* **2016**, *208* (1), 1–3.
- [30] Kametani, F.; Hasegawa, M. Reconsideration of Amyloid Hypothesis and Tau Hypothesis in Alzheimer's Disease. *Front. Neurosci.* **2018**, *12* (JAN), 1–11.
- [31] Canter, R. G.; Penney, J.; Tsai, L.; States, U. The Road to Restoring Neural Circuits for the Treatment of Alzheimer ' S Disease. *Nature* **2016**, *539*, 187–196.
- [32] Gosztyla, M. L.; Brothers, H. M.; Robinson, S. R. Alzheimer's Amyloid- β Is an Antimicrobial Peptide: A Review of the Evidence. *J. Alzheimer's Dis.* **2018**, *62* (4), 1495–1506.
- [33] Paris, D.; Townsend, K.; Quadros, A.; Humphrey, J.; Sun, J.; Brem, S.; Wotoczek-Obadia, M.; DelleDonne, A.; Patel, N.; Obregon, D. F.; et al. Inhibition of Angiogenesis by Abeta Peptides. *Angiogenesis* **2004**, *7* (1), 75–85.

- [34] Brothers, H. M.; Gosztyla, M. L.; Robinson, S. R. The Physiological Roles of Amyloid- β Peptide Hint at New Ways to Treat Alzheimer's Disease. *Front. Aging Neurosci.* **2018**, *10* (APR), 1–16.
- [35] Huber, C. M.; Yee, C.; May, T.; Dhanala, A.; Mitchell, C. S. Cognitive Decline in Preclinical Alzheimer ' S Disease : Amyloid-Beta versus Tauopathy. *J. Alzheimer's Dis.* **2018**, *61*, 265–281.
- [36] Castillo-carranza, D. L.; Guerrero-mun, M. J.; Sengupta, U.; Hernandez, C.; Barrett, A. D. T.; Dineley, K.; Kaye, R. Tau Immunotherapy Modulates Both Pathological Tau and Upstream Amyloid Pathology in an Alzheimer ' S Disease Mouse Model. *J. Neurosci.* **2015**, *35* (12), 4857–4868.
- [37] Congdon, E. E.; Sigurdsson, E. M. Tau-Targeting Therapies for Alzheimer's Disease. *Nat. Rev. Neurol.* **2018**, *14*, 399–415.
- [38] Laurent, C.; Bu, L.; Blum, D. Tau and Neuroinflammation : What Impact for Alzheimer ' S Disease and Tauopathies ? *Biomed. J. J.* **2018**, *41*, 21–33.
- [39] Manczak, M.; Reddy, P. H. RNA Silencing of Genes Involved in Alzheimer's Disease Enhances Mitochondrial Function and Synaptic Activity. *NIH Public Access* **2013**, *1832* (12), 1–26.
- [40] Hart, N. J.; Koronyo, Y.; Black, K. L.; Koronyo-Hamaoui, M. Ocular Indicators of Alzheimer's: Exploring Disease in the Retina. *Acta Neuropathol.* **2016**, *132* (6), 767–787.
- [41] Amtul, Z. Why Therapies for Alzheimer ' S Disease Do Not Work : Do We Have Consensus over the Path to Follow ? *Ageing Res. Rev.* **2016**, *25*, 70–84.
- [42] Koric, L.; Guedj, E.; Habert, M. O.; Semah, F.; Branger, P.; Payoux, P.; Jeune, F. Le. Molecular Imaging in the Diagnosis of Alzheimer ' S Disease and Related Disorders. *Rev. Neurol. (Paris).* **2016**, *172*, 725–734.
- [43] Muhammad, S.; Bierhaus, A.; Schwaninger, M. Reactive Oxygen Species in Diabetes-Induced Vascular Damage, Stroke, and Alzheimer's Disease. *J. Alzheimer's Dis.* **2009**, *16* (4), 775–785.
- [44] Sampson, E. L.; Jenagaratnam, L.; McShane, R. Metal Protein Attenuating Compounds for the

Treatment of Alzheimer's Dementia. *Eur. PMC Funders Gr.* **2014**, *5*, 1–23.

- [45] Panza, F.; Seripa, D.; Solfrizzi, V.; Imbimbo, B. P.; Leo, A.; Sardone, R.; Gagliardi, G.; Lofano, L.; Creanza, B. C.; Bisceglia, P.; et al. Expert Opinion on Emerging Drugs Emerging Drugs to Reduce Abnormal β -Amyloid Protein in Alzheimer ' S Disease Patients. *Expert Opin. Emerg. Drugs* **2016**, *21* (4), 377–391.
- [46] Tampi, R. R.; van Dyck, C. H. Memantine: Efficacy and Safety in Mild-to-Severe Alzheimer's Disease. *Neuropsychiatr. Dis. Treat.* **2007**, *3* (2), 245–258.
- [47] Cummings, J.; Lee, G.; Mortsdorf, T.; Ritter, A.; Zhong, K. Alzheimer's Disease Drug Development Pipeline: 2017. *Alzheimer's Dement. Transl. Res. Clin. Interv.* **2017**, *3* (3), 367–384.
- [48] van Dyck, C. H. Anti-Amyloid- β Monoclonal Antibodies for Alzheimer's Disease: Pitfalls and Promise. *Biol. Psychiatry* **2018**, *83* (4), 311–319.
- [49] Zhou, X.; Li, Y.; Shi, X.; Ma, C. An Overview on Therapeutics Attenuating Amyloid β Level in Alzheimer ' S Disease : Targeting Neurotransmission , Inflammation , Oxidative Stress and Enhanced Cholesterol Levels. **2016**, *8* (2), 246–269.
- [50] Wen, M. M. Getting miRNA Therapeutics into the Target Cells for Neurodegenerative Diseases : A Mini-Review. **2016**, *9* (November), 1–7.
- [51] Patel, M. M.; Goyal, B. R.; Bhadada, S. V.; Bhatt, J. S.; Amin, A. F. Getting into the Brain Approaches to Enhance Brain Drug Delivery. *CNS Drugs* **2009**, *23* (1), 35–58.
- [52] WILLIAM, M. Regulation of Blood–Brain Barrier Permeability. *Microcirculation* **2001**, *8* (2), 89–104.
- [53] Tajés, M.; Ramos-Fernández, E.; Weng-Jiang, X.; Bosch-Morató, M.; Guivernau, B.; Eraso-Pichot, A.; Salvador, B.; Fernández-Busquets, X.; Roquer, J.; Muñoz, F. J. The Blood-Brain Barrier: Structure, Function and Therapeutic Approaches to Cross It. *Mol. Membr. Biol.* **2014**, *31* (5), 152–167.
- [54] Verheggen, I. C. M.; Van Boxtel, M. P. J.; Verhey, F. R. J.; Jansen, J. F. A.; Backes, W. H.

- Interaction between Blood-Brain Barrier and Glymphatic System in Solute Clearance. *Neurosci. Biobehav. Rev.* **2018**, *90* (March), 26–33.
- [55] Das, S.; Carnicer-Lombarte, A.; Fawcett, J. W.; Bora, U. Bio-Inspired Nano Tools for Neuroscience. *Prog. Neurobiol.* **2016**, *142*, 1–22.
- [56] Guo, T.; Lin, M.; Huang, J.; Zhou, C.; Tian, W.; Yu, H.; Jiang, X.; Ye, J.; Shi, Y.; Xiao, Y.; et al. The Recent Advances of Magnetic Nanoparticles in Medicine. *J. Nanomater.* **2018**, *2018*, 1–8.
- [57] Schwartz, S. Unmet Needs in Developing Nanoparticles for Precision Medicine. *Nanomedicine* **2017**, *12* (4), 271–274.
- [58] Chaudhry, Q.; Scotter, M.; Blackburn, J.; Ross, B.; Boxall, A.; Castle, L.; Aitken, R.; Watkins, R. Applications and Implications of Nanotechnologies for the Food Sector. *Food Addit. Contam. - Part A Chem. Anal. Control. Expo. Risk Assess.* **2008**, *25* (3), 241–258.
- [59] Zaman, M.; Ahmad, E.; Qadeer, A.; Rabbani, G.; Hasa. Nanoparticles in Relation to Peptide and Protein Aggregation. *Int. J. Nanomedicine* **2014**, *9* (March), 899–912.
- [60] Seku, K.; Ganapuram, B. R.; Pejjai, B.; Kotu, G. M.; Narasimha, G. Hydrothermal Synthesis of Copper Nanoparticles, Characterization and Their Biological Applications. *Int. J. Nano Dimens.* **2018**, *9* (1), 7–14.
- [61] Mohammed Fayaz, A.; Balaji, K.; Kalaichelvan, P. T.; Venkatesan, R. Fungal Based Synthesis of Silver Nanoparticles-An Effect of Temperature on the Size of Particles. *Colloids Surfaces B Biointerfaces* **2009**, *74* (1), 123–126.
- [62] Veith, G. M.; Lupini, A. R.; Dudney, N. J. Role of pH in the Formation of Structurally Stable and Catalytically Active TiO₂-Supported Gold Catalysts. *J. Phys. Chem. C* **2009**, *113* (1), 269–280.
- [63] Belanova, A. A.; Zolotukhin, P. V.; Gavalas, N.; Makarenko, Y. M.; Belousova, M. M.; Soldatov, A. V. Physicochemical Properties of Magnetic Nanoparticles: Implications for Biomedical Applications in Vitro and in Vivo. *Oncol. Res. Treat.* **2018**, *41*, 139–143.
- [64] Chan, H.; Yamada, S.; Chan, H. Nanodrugs: Pharmacokinetics and Safety. *Int. J. Nanomedicine* **2014**, *9*, 1025–1037.

- [65] Carlyle, W. C.; McClain, J. B.; Tzafirri, A. R.; Bailey, L.; Brett, G.; Markham, P. M.; Stanley, J. R. L.; Edelman, E. R.; Sciences, C. B.; Technologies, E.; et al. Safety of Nanoparticles in Medicine. *Curr. Drug Targets* **2015**, *162* (3), 561–567.
- [66] Sufian, M. M.; Khattak, J. Z. K.; Yousaf, S.; Rana, M. S. Safety Issues Associated with the Use of Nanoparticles in Human Body. *Photodiagnosis Photodyn. Ther.* **2017**, *19* (April), 67–72.
- [67] Lin, Z.; Monteiro-Riviere, N. A.; Riviere, J. E. Pharmacokinetics of Metallic Nanoparticles. *Wiley Interdiscip. Rev. Nanomedicine Nanobiotechnology* **2015**, *7* (2), 189–217.
- [68] Longmire, M.; L. Choyke, P.; Kobayashi, H. Clearance Properties of Nano-Sized Particles and Molecules as Imaging Agents: Considerations and Caveats. *Nanomedicine* **2008**, *3* (5), 703–717.
- [69] Zhang, B.; Misak, H.; Dhanasekaran, P. S.; Kalla, D.; Asmatulu, R. Environmental Impacts of Nanotechnology and Its Products. *Am. Soc. Eng. Educ.* **1845**, *1*, 1–9.
- [70] Ray, P. C.; Fu, P. P. Toxicity and Environmental Risks of Nanomaterials: Challenges and Future Needs Paresh. *J. Env. Sci Heal. C Env. Carcinog Ecotoxicol Rev.* **2009**, *27* (1), 1–35.
- [71] Mallick, S.; Choi, J. S. Liposomes: Versatile and Biocompatible Nanovesicles for Efficient Biomolecules Delivery. *J. Nanosci. Nanotechnol.* **2014**, *14* (1), 755–765.
- [72] Lin, L. N.; Liu, Q.; Song, L.; Liu, F. F.; Sha, J. X. Recent Advances in Nanotechnology Based Drug Delivery to the Brain. *Cytotechnology* **2010**, *62* (5), 377–380.
- [73] Gunay, M. S.; Ozer, A. Y.; Erdogan, S.; Bodard, S.; Baysal, I.; Gulhan, Z.; Guilloteau, D.; Chalon, S. Development of Nanosized, Pramipexole-Encapsulated Liposomes and Niosomes for the Treatment of Parkinson's Disease. *J. Nanosci. Nanotechnol.* **2017**, *17* (8), 5155–5167.
- [74] Balducci, C.; Mancini, S.; Minniti, S.; La Vitola, P.; Zotti, M.; Sancini, G.; Mauri, M.; Cagnotto, A.; Colombo, L.; Fiordaliso, F.; et al. Multifunctional Liposomes Reduce Brain β -Amyloid Burden and Ameliorate Memory Impairment in Alzheimer's Disease Mouse Models. *J. Neurosci.* **2014**, *34* (42), 14022–14031.
- [75] Sercombe, L.; Veerati, T.; Moheimani, F.; Wu, S. Y.; Sood, A. K.; Hua, S. Advances and Challenges of Liposome Assisted Drug Delivery. *Front. Pharmacol.* **2015**, *6* (DEC), 1–13.

- [76] Mohammed, S. J.; Salih, A. K.; Omer, K. M. Preparation and Characterization of Organic Nanoparticles of Oxadiazole Derivative in Aqueous Media. *J. Nat. Sci. Res.* **2014**, *4* (21), 81–86.
- [77] Chopra, M.; Jain, R.; Dewangan, A. K.; Varkey, S.; Mazumder, S. Design of Curcumin Loaded Polymeric Nanoparticles-Optimization, Formulation and Characterization. *J. Nanosci. Nanotechnol.* **2016**, *16* (9), 9432–9442.
- [78] Kim, M. J.; Rehman, S. U.; Amin, F. U.; Kim, M. O. Enhanced Neuroprotection of Anthocyanin-Loaded PEG-Gold Nanoparticles against A β 1-42-Induced Neuroinflammation and Neurodegeneration via the NF-KB /JNK/GSK3 β Signaling Pathway. *Nanomedicine Nanotechnology, Biol. Med.* **2017**, *13* (8), 2533–2544.
- [79] Geng, J.; Li, M.; Wu, L.; Chen, C.; Qu, X. Mesoporous Silica Nanoparticle-Based H₂O₂ Responsive Controlled-Release System Used for Alzheimer's Disease Treatment. *Adv. Healthc. Mater.* **2012**, *1* (3), 332–336.
- [80] Marslin, G.; Filipe, B.; Cardoso, C.; Franklin, G.; Alberto, J.; Martins, R.; Jorge, C.; Silva, R.; Ferreira, A.; Gomes, C.; et al. Curcumin Encapsulated into Increases Cellular Uptake and Neuroprotective Effect in Glioma Curcumin Encapsulated into Methoxy Poly (Ethylene Glycol) Poly (ϵ -Caprolactone) Nanoparticles Increases Cellular Uptake and Neuroprotective Effect in Glioma Cel. *Planta Med* **2016**, *83*, 434–444.
- [81] Elnaggar, Y. S. R.; Etman, S. M.; Abdelmonsif, D. A.; Abdallah, O. Y. Intranasal Piperine-Loaded Chitosan Nanoparticles as Brain-Targeted Therapy in Alzheimer's Disease: Optimization, Biological Efficacy, and Potential Toxicity. *J. Pharm. Sci.* **2015**, *104* (10), 3544–3556.
- [82] Luppi, B.; Bigucci, F.; Corace, G.; Delucca, A.; Cerchiara, T.; Sorrenti, M.; Catenacci, L.; Di Pietra, A. M.; Zecchi, V. Albumin Nanoparticles Carrying Cyclodextrins for Nasal Delivery of the Anti-Alzheimer Drug Tacrine. *Eur. J. Pharm. Sci.* **2011**, *44* (4), 559–565.
- [83] Gregori, M. Nanomedicine for the Treatment of Alzheimer ' S Disease. **2015**, *10*, 1203–1218.
- [84] Yusuf, M.; Khan, M.; Khan, R. A.; Ahmed, B. Preparation, Characterization, in Vivo and Biochemical Evaluation of Brain Targeted Piperine Solid Lipid Nanoparticles in an Experimentally Induced Alzheimer ' S Disease Model. *J. Drug Target.* **2013**, *21* (September

2012), 300–311.

- [85] Prades, R.; Guerrero, S.; Araya, E.; Molina, C.; Salas, E.; Zurita, E.; Selva, J.; Egea, G.; López-iglesias, C.; Teixidó, M.; et al. Biomaterials Delivery of Gold Nanoparticles to the Brain by Conjugation with a Peptide That Recognizes the Transferrin Receptor. *2012*, *33*, 7194–7205.
- [86] Alvarez-erviti, L.; Seow, Y.; Yin, H.; Betts, C.; Lakhali, S.; Wood, M. J. A. Delivery of siRNA to the Mouse Brain by Systemic Injection of Targeted Exosomes. *Nat. Biotechnol.* **2011**, *29* (4), 341–347.
- [87] Saha, S.; Adhikary, A.; Bhattacharyya, P.; Das, T.; Sa, G. Daeth by Design: Where Curcumin Sensitizes Drug Resistant Tumors. *Anticancer Res.* **2012**, *32*, 2567–2584.
- [88] Chi, H. P.; Eun, R. H.; Park, S.; Kim, H. K.; Chul, H. Y. The Inhibitory Mechanism of Curcumin and Its Derivative against β -catenin/Tcf Signaling. *FEBS Lett.* **2005**, *579* (13), 2965–2971.
- [89] Prasad, S.; Aggarwal, B. B. Turmeric, the Golden Spice: From Traditional Medicine to Modern Medicine. In *Turmeric, the Golden Spice: From Traditional Medicine to Modern Medicine*; IFF, B., S. W.-G., Eds.; Boca Raton (FL), 2011.
- [90] Feng, T.; Wei, Y.; Lee, R. J.; Zhao, L. Liposomal Curcumin and Its Application in Cancer. *Int. J. Nanomedicine* **2017**, *12*, 6027–6044.
- [91] Inoue, K.; Nomura, C.; Ito, S.; Nagatsu, A.; Hino, T.; Oka, H. Purification of Curcumin, Demethoxycurcumin, and Bisdemethoxycurcumin by High-Speed Countercurrent Chromatography. *J. Agric. Food Chem.* **2008**, *56* (20), 9328–9336.
- [92] Mahmood, K.; Zia, K. M.; Zuber, M.; Salman, M.; Anjum, M. N. Recent Developments in Curcumin and Curcumin Based Polymeric Materials for Biomedical Applications: A Review. *Int. J. Biol. Macromol.* **2015**, *81*, 877–890.
- [93] Yang, F.; Lim, G. P.; Begum, A. N.; Ubeda, O. J.; Simmons, M. R.; Ambegaokar, S. S.; Chen, P.; Kaye, R.; Glabe, C. G.; Frautschi, S. A.; et al. Curcumin Inhibits Formation of Amyloid β Oligomers and Fibrils, Binds Plaques, and Reduces Amyloid in Vivo. *J. Biol. Chem.* **2005**, *280* (7), 5892–5901.

- [94] Li, L.; Ahmed, B.; Mehta, K.; Kurzrock, R. Liposomal Curcumin with and without Oxaliplatin: Effects on Cell Growth, Apoptosis, and Angiogenesis in Colorectal Cancer. *Mol. Cancer Ther.* **2007**, *6* (4), 1276–1282.
- [95] Akbar, M. U.; Zia, K. M.; Nazir, A.; Iqbal, J.; Ejaz, S. A.; Akash, M. S. H. Pluronic-Based Mixed Polymeric Micelles Enhance the Therapeutic Potential of Curcumin. *AAPS PharmSciTech* **2018**, *19* (6), 2719–2739.
- [96] Woraphatphadung, T.; Sajomsang, W.; Rojanarata, T.; Ngawhirunpat, T.; Tonglairoum, P.; Opanasopit, P. Development of Chitosan-Based pH-Sensitive Polymeric Micelles Containing Curcumin for Colon-Targeted Drug Delivery. *AAPS PharmSciTech* **2017**, *19* (3), 991–1001.
- [97] Muddineti, O. S.; Kumari, P.; Ghosh, B.; Biswas, S. Transferrin-Modified Vitamin-E / Lipid Based Polymeric Micelles for Improved Tumor Targeting and Anticancer Effect of Curcumin. *Pharm. Res.* **2018**, *35* (97), 1–14.
- [98] Chen, F. P.; Li, B. S.; Tang, C. H. Nanocomplexation of Soy Protein Isolate with Curcumin: Influence of Ultrasonic Treatment. *Food Res. Int.* **2015**, *75*, 157–165.
- [99] Samuelsson, E.; Shen, H.; Blanco, E.; Ferrari, M.; Wolfram, J. Contribution of Kupffer Cells to Liposome Accumulation in the Liver. *Colloids Surfaces B Biointerfaces* **2017**, *158*, 356–362.
- [100] Ginn, S. L.; Amaya, A. K.; Alexander, I. E.; Edelstein, M.; Abedi, M. R. Gene Therapy Clinical Trials Worldwide To 2017 - an Update. *J. Gene Med.* **2018**, *20* (January), e3015.
- [101] Robbins, P. D.; Ghivizzani, S. C. Viral Vectors for Gene Therapy. *Pharmacol. Ther.* **1998**, *80* (1), 35–47.
- [102] Cucchiaroni, M. Human Gene Therapy: Novel Approaches to Improve the Current Gene Delivery Systems. *Discov. Med.* **2016**, *21* (118), 495–506.
- [103] Lorenzer, C.; Dirin, M.; Winkler, A. M.; Baumann, V.; Winkler, J. Going beyond the Liver: Progress and Challenges of Targeted Delivery of siRNA Therapeutics. *J. Control. Release* **2015**, *203*, 1–15.
- [104] Ganbold, T.; Baigude, H. Design of Mannose-Functionalized Curdlan Nanoparticles for Macrophage-Targeted siRNA Delivery. *ACS Appl. Mater. Interfaces* **2018**, *10* (17), 14463–

14474.

- [105] Zhang, H.; Wang, Y.; Bai, M.; Wang, J.; Zhu, K.; Liu, R.; Ge, S.; Li, J. L.; Ning, T.; Deng, T.; et al. Exosomes Serve as Nanoparticles to Suppress Tumor Growth and Angiogenesis in Gastric Cancer by Delivering Hepatocyte Growth Factor siRNA. *Cancer Sci.* **2018**, *109* (3), 629–641.
- [106] Leng, O.; Woodle, M. C.; Lu, P. Y.; Mixson, A. J. Advances in Systemic siRNA Delivery. *Drugs Future* **2009**, *34* (9), 721–737.
- [107] Botulinum, R. I.; Study, R. Effect of Surface Properties on Liposomal siRNA Delivery. **2014**, *4* (1), 139–148.
- [108] Schneider, A.; Simons, M. Exosomes: Vesicular Carriers for Intercellular Communication in Neurodegenerative Disorders. *Cell Tissue Res.* **2013**, *352* (1), 33–47.
- [109] Barile, L.; Vassalli, G. Exosomes: Therapy Delivery Tools and Biomarkers of Diseases. *Pharmacol. Ther.* **2017**, *174*, 63–78.
- [110] Théry, C.; Zitvogel, L.; Amigorena, S. Exosomes: Composition, Biogenesis and Function. *Nat. Rev. Immunol.* **2002**, *2* (8), 569–579.
- [111] Clayton, A. Adhesion and Signaling by B Cell-Derived Exosomes: The Role of Integrins. *FASEB J.* **2004**, *22* (2), 1–22.
- [112] McKelvey, K. J.; Powell, K. L.; Ashton, A. W.; Morris, J. M.; McCracken, S. A. Exosomes: Mechanisms of Uptake. *J. Circ. Biomarkers* **2015**, *4* (7), 1.
- [113] Mittelbrunn, M.; Gutiérrez-Vázquez, C.; Villarroya-Beltri, C.; González, S.; Sánchez-Cabo, F.; González, M. Á.; Bernad, A.; Sánchez-Madrid, F. Unidirectional Transfer of microRNA-Loaded Exosomes from T Cells to Antigen-Presenting Cells. *Nat. Commun.* **2011**, *2* (282), 1–10.
- [114] He, C.; Zheng, S.; Luo, Y.; Wang, B. Exosome Theranostics: Biology and Translational Medicine. *Theranostics* **2018**, *8* (1), 237–255.
- [115] Ju, S.; Mu, J.; Dokland, T.; Zhuang, X.; Wang, Q.; Jiang, H.; Xiang, X.; Deng, Z. Bin; Wang, B.; Zhang, L.; et al. Grape Exosome-like Nanoparticles Induce Intestinal Stem Cells and Protect Mice from DSS-Induced Colitis. *Mol. Ther.* **2013**, *21* (7), 1345–1357.

- [116] Muldoon, M. F.; Ryan, C. M.; Yao, J. K.; Conklin, S. M.; Manuck, S. B.; Hall, O. E. Grapefruit-Derived Nanovectors Use an Activated Leukocyte Trafficking Pathway to Deliver Therapeutic Agents to Inflammatory Tumor Sites. *Cancer Res.* **2015**, *75* (12), 2520–2529.
- [117] Zhao, Z.; Yu, S.; Li, M.; Gui, X.; Li, P. Isolation of Exosome-Like Nanoparticles and Analysis of MicroRNAs Derived from Coconut Water Based on Small RNA High-Throughput Sequencing. *J. Agric. Food Chem.* **2018**, *66* (11), 2749–2757.
- [118] Raimondo, S.; Naselli, F.; Fontana, S.; Monteleone, F.; Dico, A. Lo; Saieva, L.; Zito, G.; Flugy, A.; Manno, M.; Di Bella, M. A.; et al. Citrus Limon-Derived Nanovesicles Inhibit Cancer Cell Proliferation and Suppress CML Xenograft Growth by Inducing TRAIL-Mediated Cell Death. *Oncotarget* **2015**, *6* (23), 19514–19527.
- [119] Mu, J.; Zhuang, X.; Wang, Q.; Jiang, H.; Deng, Z. Bin; Wang, B.; Zhang, L.; Kakar, S.; Jun, Y.; Miller, D.; et al. Interspecies Communication between Plant and Mouse Gut Host Cells through Edible Plant Derived Exosome-like Nanoparticles. *Mol. Nutr. Food Res.* **2014**, *58* (7), 1561–1573.
- [120] Lunavat, T. R.; Jang, S. C.; Nilsson, L.; Park, H. T.; Repiska, G.; Lässer, C.; Nilsson, J. A.; Gho, Y. S.; Lötvall, J. RNAi Delivery by Exosome-Mimetic Nanovesicles – Implications for Targeting c-Myc in Cancer. *Biomaterials* **2016**, *102*, 231–238.
- [121] Jang, S. C.; Kim, O. Y.; Yoon, C. M.; Choi, D. S.; Roh, T. Y.; Park, J.; Nilsson, J.; Lötvall, J.; Kim, Y. K.; Gho, Y. S. Bioinspired Exosome-Mimetic Nanovesicles for Targeted Delivery of Chemotherapeutics to Malignant Tumors. *ACS Nano* **2013**, *7* (9), 7698–7710.
- [122] Bryniarski, K.; Ptak, W.; Jayakumar, A.; Püllmann, K. Antigen Specific Antibody Coated Exosome-like Nanovesicles Deliver Suppressor T Cell miRNA-150 to Effector T Cells in Contact Sensitivity. *Heal. Psychol.* **2009**, *119* (11), 2658–2666.
- [123] Chen, F.; Ma, M.; Wang, J.; Wang, F.; Chern, S. X.; Zhao, E. R.; Jhunjhunwala, A.; Darmadi, S.; Chen, H.; Jokerst, J. V. Exosome-like Silica Nanoparticles: A Novel Ultrasound Contrast Agent for Stem Cell Imaging. *Nanoscale* **2017**, *9* (1), 402–411.
- [124] Zolnik, B. S.; González-Fernández, Á. ´; Sadrieh, N.; Dobrovolskaia, M. A. Minireview: Nanoparticles and the Immune System. *Endocrinology* **2010**, *151* (2), 458–465.

- [125] Dulbecco, P.; Savarino, V. Therapeutic Potential of Curcumin in Digestive Diseases. *World J. Gastroenterol.* **2013**, *19* (48), 9256–9270.
- [126] Hassan, P. A.; Rana, S.; Verma, G. Making Sense of Brownian Motion: Colloid Characterization by Dynamic Light Scattering. *Langmuir* **2015**, *31* (1), 3–12.
- [127] Zhou, W.; Su, M.; Cai, X. Advances in Nanoparticle Sizing in Suspensions: Dynamic Light Scattering and Ultrasonic Attenuation Spectroscopy. *KONA Powder Part. J.* **2017**, *34*, 168–182.
- [128] Riss, T. L.; Moravec, R. A.; Niles, A. L.; Duellman, S.; Benink, H. A.; Worzella, T. J.; Minor, L. Cell Viability Assays. *Assay Guid. Man.* **2013**, *114* (8), 785–796.
- [129] Jaafar-Maalej, C.; Diab, R.; Andrieu, V.; Elaissari, A.; Fessi, H. Ethanol Injection Method for Hydrophilic and Lipophilic Drug-Loaded Liposome Preparation. *J. Liposome Res.* **2010**, *20* (3), 228–243.
- [130] Pons, M.; Foradada, M.; Estelrich, J. Liposomes Obtained by the Ethanol Injection Method. *Int. J. Pharm.* **1993**, *95* (1–3), 51–56.
- [131] Charcosset, C.; Juban, A.; Valour, J. P.; Urbaniak, S.; Fessi, H. Preparation of Liposomes at Large Scale Using the Ethanol Injection Method: Effect of Scale-up and Injection Devices. *Chem. Eng. Res. Des.* **2015**, *94* (September), 508–515.
- [132] Azmi, N. H.; Ismail, N.; Imam, M. U.; Ismail, M. Ethyl Acetate Extract of Germinated Brown Rice Attenuates Hydrogen Peroxide-Induced Oxidative Stress in Human SH-SY5Y Neuroblastoma Cells: Role of Anti-Apoptotic, pro-Survival and Antioxidant Genes. *BMC Complement. Altern. Med.* **2013**, *13* (1), 1.
- [133] Stubičar, N.; Matejaš, J.; Zipper, P.; Wilfing, R. Size, Shape and Internal Structure of Triton X-100 Micelles Determined by Light and Small-Angle X-Ray Scattering Techniques. In *Surfactants in Solution*; Mittal, K. L., Ed.; Springer US: Boston, MA, 1989; pp 181–195.
- [134] Tam, Y. Y. C.; Chen, S.; Cullis, P. R. Advances in Lipid Nanoparticles for siRNA Delivery. *Pharmaceutics* **2013**, *5* (3), 498–507.
- [135] Ng, Z. Y.; Wong, J. Y.; Panneerselvam, J.; Madheswaran, T.; Kumar, P.; Pillay, V.; Hsu, A.;

- Hansbro, N.; Bebawy, M.; Wark, P.; et al. Assessing the Potential of Liposomes Loaded with Curcumin as a Therapeutic Intervention in Asthma. *Colloids Surfaces B Biointerfaces* **2018**, *172* (August), 51–59.
- [136] Taylor, M.; Moore, S.; Mourtas, S.; Niarakis, A.; Re, F.; Zona, C.; Ferla, B. La; Nicotra, F.; Masserini, M.; Antimisiaris, S. G.; et al. Effect of Curcumin-Associated and Lipid Ligand-Functionalized Nanoliposomes on Aggregation of the Alzheimer's A β Peptide. *Nanomedicine Nanotechnology, Biol. Med.* **2011**, *7* (5), 541–550.
- [137] Li, R.; Deng, L.; Cai, Z.; Zhang, S.; Wang, K.; Li, L.; Ding, S.; Zhou, C. Liposomes Coated with Thiolated Chitosan as Drug Carriers of Curcumin. *Mater. Sci. Eng. C* **2017**, *80*, 156–164.
- [138] Rahman, S.; Telny, T.; Ravi, T.; Kuppusamy, S. Role of Surfactant and pH in Dissolution of Curcumin. *Indian J. Pharm. Sci.* **2009**, *71* (2), 139.
- [139] Mofazzal Jahromi, M. A.; Al-Musawi, S.; Pirestani, M.; Fasihi Ramandi, M.; Ahmadi, K.; Rajayi, H.; Mohammad Hassan, Z.; Kamali, M.; Mirnejad, R. Curcumin-Loaded Chitosan Tripolyphosphate Nanoparticles as a Safe, natural and Effective Antibiotic Inhibits the Infection of Staphylococcus aureus and Pseudomonas Aeruginosa in Vivo. *Iran. J. Biotechnol.* **2014**, *12* (3), 1–8.
- [140] Romøren, K.; Thu, B. J.; Bols, N. C.; Evensen, Ø. Transfection Efficiency and Cytotoxicity of Cationic Liposomes in Salmonid Cell Lines of Hepatocyte and Macrophage Origin. *Biochim. Biophys. Acta - Biomembr.* **2004**, *1663* (1–2), 127–134.
- [141] Simak, J. The Effects of Engineered Nanomaterials on the Plasma Coagulation System Disclaimer: *Handb. Immunol. Prop. Eng. Nanomater.* **2013**, *6*, 263–291.
- [142] Saffari, M.; Shirazi, F. H.; Oghabian, M. A.; Moghimi, H. R. Preparation and in-Vitro Evaluation of an Antisense-Containing Cationic Liposome against Non-Small Cell Lung Cancer: A Comparative Preparation Study. *Iran. J. Pharm. Res.* **2013**, *12* (SUPPL.), 1–8.
- [143] Li, L.; Ahmed, B.; Mehta, K.; Kurzrock, R. Liposomal Curcumin with and without Oxaliplatin: Effects on Cell Growth, Apoptosis, and Angiogenesis in Colorectal Cancer. *Mol. Cancer Ther.* **2007**, *6* (4), 1276–1282.

- [144] Banderali, U.; Belke, D.; Singh, A.; Jayanthan, A.; Giles, W. R.; Narendran, A. Curcumin Blocks Kv11.1 (Erg) Potassium Current and Slows Proliferation in the Infant Acute Monocytic Leukemia Cell Line THP-1. *Cell. Physiol. Biochem.* **2011**, *28* (6), 1169–1180.
- [145] Woo, J.-H.; Kim, Y.-H.; Choi, Y.-J.; Kim, D.-G.; Lee, K.-S.; Bae, J. H.; Min, D. S.; Chang, J.-S.; Jeong, Y.-J.; Lee, Y. H.; et al. Molecular Mechanisms of Curcumin-Induced Cytotoxicity: Induction of Apoptosis through Generation of Reactive Oxygen Species, down-Regulation of Bcl-XL and IAP, the Release of Cytochrome c and Inhibition of Akt. *Carcinogenesis* **2003**, *24* (7), 1199–1208.
- [146] Daverey, A.; Agrawal, S. K. Curcumin Alleviates Oxidative Stress and Mitochondrial Dysfunction in Astrocytes. *Neuroscience* **2016**, *333*, 92–103.
- [147] Yin, W.; Zhang, X.; Shi, X.; Li, Y. Curcumin Protects SH-SY5Y Cells from Oxidative Stress by up-Regulating HO-1 via Phosphatidylinositol 3 Kinase/Akt/Nrf-2 and down-Regulating HO-2. *Mol. Neurodegener.* **2012**, *7* (Suppl 1), S14–S14.
- [148] Kragh-Hansen, U.; Le Maire, M.; Møller, J. V. The Mechanism of Detergent Solubilization of Liposomes and Protein-Containing Membranes. *Biophys. J.* **1998**, *75* (6), 2932–2946.
- [149] Foresta, B. de; Maire, M.; Orłowski, S.; Champeil, P.; Lund, S.; Møller, J. V.; Michelangeli, F.; Lee, A. G. Membrane Solubilization by Detergent: Use of Brominated Phospholipids To Evaluate the Detergent-Induced Changes in Ca²⁺-ATPase/Lipid Interaction. *Biochemistry* **1989**, *28* (6), 2558–2567.
- [150] Dabbas, S.; Kaushik, R. R.; Dandamudi, S.; Kuesters, G. M.; Campbell, R. B. Importance of the Liposomal Cationic Lipid Content and Type in Tumor Vascular Targeting: Physicochemical Characterization and in Vitro Studies Using Human Primary and Transformed Endothelial Cells. *Endothel. J. Endothel. Cell Res.* **2008**, *15* (4), 189–201.
- [151] Instruments, M. *Malvern Zetasizer ZS DLS User Manual*; Malvern, 2013.

5. Supplementary Data

24 H

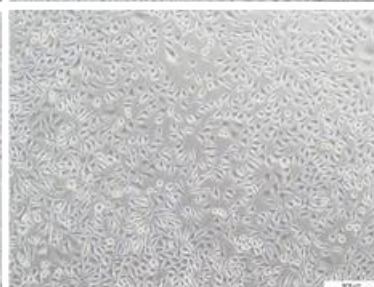
48 H

72 H

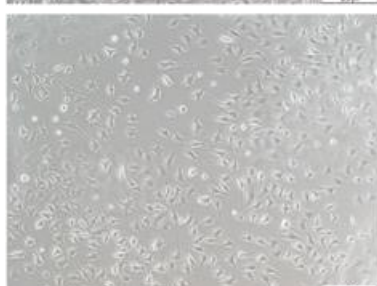
Liposomes without DODAP
(C= 8×10^{-7} M)



Liposomes without DODAP
(C= 5×10^{-3} M)



Liposomes with DODAP
(C= $6,4 \times 10^{-7}$ M)



Liposomes with DODAP
(C= 4×10^{-3} M)

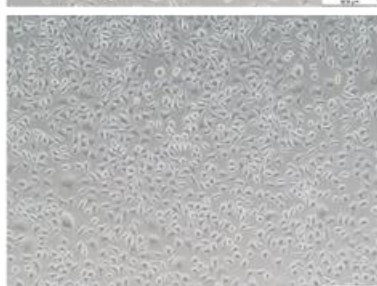


Figure 29: L929 cell morphology after 24 h of incubation with the liposomes.